CHAPTER ONE

INTRODUCTION

1 INTRODUCTION

1.1 General Overview

Advances in nanomaterials are helping to develop electrochemical sensors with increased sensitivity that can be extensively applied to a wide variety of analytical problems including clinical, medicinal, drug discovery, food and environmental areas. Electrochemical methods have proven to be more cost effective, simple, user friendly, portable, and faster than other analytical methods. Therefore, there is a need to design and develop high-speed and high-performance electrochemical sensors that can hold an outstanding ability among analytical devices available for environmental applications. However, the success of electrochemical sensing device is determined by (i) the electrode, (iii) the construction technique (which determines its stability or shelf life and reliability) and (ii) the electrocatalyst. Over the past decade, carbon nanotubes and phthalocyanine complexes have received considerable attention because of their unique physico-chemical and electronic properties. However, their smart integration in electrochemical sensing is hugely under-explored. It is also anticipated that the interaction of phthalocyanine complexes with monolayer-protected clusters of gold nanoparticles will provide a combination that will revolutionize their applications as electrocatalysts in electrochemical sensors.

This project describes the electron transport and electrocatalytic behaviour of single-walled carbon nanotubes (SWCNTs), monolayer-protected clusters of gold nanoparticles (MPCAuNPs) independently and phthalocyanine complexes immobilized on a thiol based gold substrate towards the detection of epinephrine and hydrogen peroxide.

Aim of Dissertation:

i. To characterize redox-active phthalocyanine complexes integrated with (i) Single-walled carbon nanotube and (ii) MPCAuNPs spectroscopic, microscopic and electrochemical techniques.

ii. To modify bare gold electrode with self assembled mono and multi-layers of SWCNT, MPCAuNPs and MPc complexes, and establish their electrochemical properties.

iii. To investigate the electrocatalytic ability of modified electrodes towards the detection of epinephrine and hydrogen peroxide.

This introductory section provides a general overview of electrochemistry, electrochemical techniques, electrode modification processes, carbon nanotubes, phthalocyanine complexes, monolayer-protected clusters of gold nanoparticles, relevant analytes such as epinephrine and hydrogen peroxide as well as microscopic techniques. In chapter two the procedure adopted for the experiment is provided. Chapter three discusses the results obtained.

1.2 Electrochemistry : An Overview

1.2.1 Basic Concepts

Electrochemistry may simply be defined as the study of chemical reactions used to produce electric power or, alternatively, the use of electricity to effect chemical processes or systems [1,2]. Hence, electrochemistry can be seen as the relationship between electricity and chemistry, namely the measurements of electric quantities, such as current, potential, and charge, and their relationship to chemical parameters. These chemical reactions involving the transfer of electrons to and from a molecule or ion are often referred to as redox (reduction/oxidation) reactions. The use of electrochemistry for analytical purposes has found a wide range of applications in industrial quality control, metallurgy, geology, pharmacy, medicinal chemistry, biomedical analysis and environmental monitoring [2].

Unlike many chemical measurements, which involve homogenous bulk solutions, the fundamental electrochemical reactions are heterogeneous in nature as they take place at interfaces, usually electrode-solution boundaries. The electrode creates a phase boundary that differentiates otherwise identical solute molecules; those at a distance from the electrode, and those close enough to the surface of the electrode to participate in the electron transfer process [1,2]. This section takes a closer look at some of the electroanalytical techniques and electrode processes employed in this dissertation.

1.2.1.1 Electrochemical Equilibrium: Introduction

The system represented in Equation 1.1, used to describe the electrochemical equilibrium process, reaches a state of equilibrium when an inert metal (usually platinum electrode) is added to a solution containing potassium hexacyanoferrate(II), $K_4Fe(CN)_6$, and potassium hexacyanoferrate(III), $K_3Fe(CN)_6$ dissolved in water.

$$Fe(CN)_6^{3-}\,(aq) + e^- \rightleftharpoons Fe(CN)_6^{4-}\,(aq) \qquad 1.1$$

When the state of equilibrium is reached the rate at which $Fe(CN)_6^{4-}$ gives up electrons to the electrode is exactly balanced by the rate at which electrons are released by the electrode to the $Fe(CN)_6^{3-}$ anions. The $Fe(CN)_6^{3-}$ and $Fe(CN)_6^{4-}$ anions are said to be reduced and oxidised respectively. The reaction involves the transfer of charged particles (electrons). Therefore, if the reaction lies to the right or left when equilibrium is reached a charge separation develops at the solution - electrode interface. Accordingly, an electrode potential is established at the metal electrode relative to the solution. Chemical processes, such as this example which establish electrode potentials, are referred to as potential determining equilibria [3]. Other examples where an electrochemical process is capable of forming a potential on the electrode in an aqueous medium include: (i) the hydrogen electrode, (ii) the silver|silver chloride electrode and (iii) the calomel electrode.

1.2.1.2 Electrochemical Equilibrium: Electron Transfer at the Electrode – Solution Interface

The electrode – solution interface also known as "electric double layer" is illustrated in Figure 1.1 It is the currently accepted representation [3] that was derived from the Helmholtz and Guoy-Chapman models which show the interface as a single capacitor and as a Boltzman distribution of ions respectively.

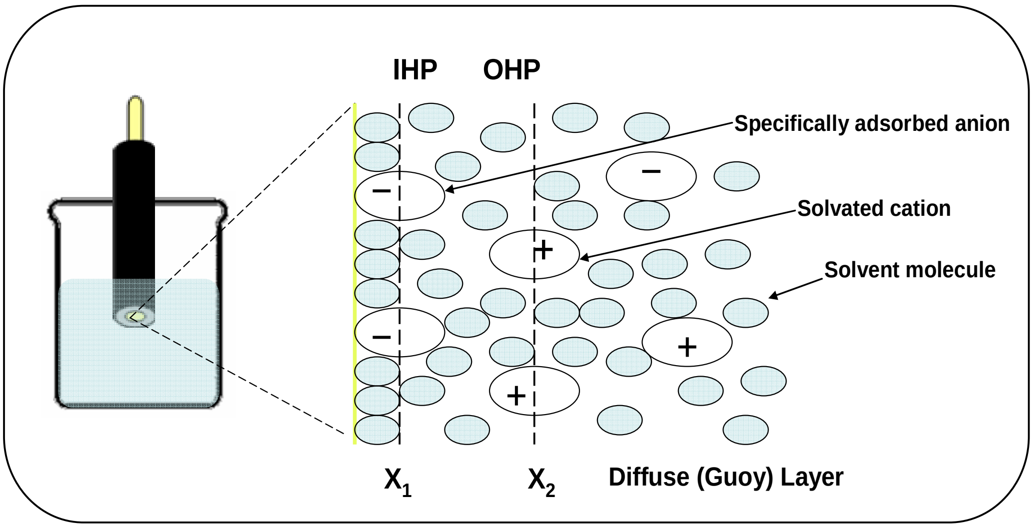

Figure 1.1: Model of the electrode – solution double layer region [3].

The electrical double layer comprises of inner layer, outer layer and the diffuse or Guoy layer. The inner layer, also referred to as, the Inner Helmholtz Plane (IHP) is area closest to the electrode surface where adsorbed ions and solvent molecules are found. The outer layer, the Outer Helmholtz Planes (OHP) is the imaginary plane passing through the solvated cations. The solvated cations undergo nonspecfic adsorption and are pulled towards the electrode surface by long range coulombic forces. Technically, the Inner and Outer Helmholtz Planes do not exist, nor can they be measured. However, the distance can be explained using the solvent molecules as well as the radius of the ions, where, the distance from the electrode surface to the IHP (X_1) is equivalent to the radius of the cation and the distance to the OHP is approximately two solvent molecules and the radius of the ion. These two layers are strongly held by the electrode and they remain at the surface even if the electrode is removed from solution. The outer most layer which extends from the OHP to the bulk is known as the diffuse or Guoy layer. The three dimensional region of scattered ions is as a result of the balance between the disorder caused by random thermal motion and the order due to electrostatic attractive and repulsive forces from the electrode surface. The presence of the electrode cannot be felt by the ion beyond this region.

1.2.1.3 Classification of Electrochemical Techniques

The flowchart represented in Figure 1.2 illustrates the classes and sub–divisions of electrochemical techniques.

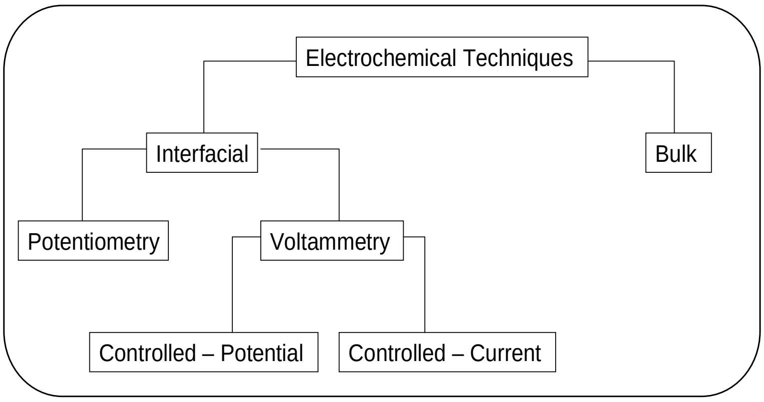

Figure 1.2: Flowchart representing Electrochemical Techniques

Bulk techniques are based on the phenomena that occur in the solution whereas interfacial techniques are based on the events occurring at the electrode–solution interface. Interfacial is sub–divided into potentiometric and voltammetric methods. Voltammetric techniques may be further divided into controlled–potential and controlled–current methods. Frequently used techniques such as voltammetry and chronoamperometry are an example of controlled–potential. It involves controlling the potential while measuring the current. The advantages of this technique include high sensitivity and selectivity towards electroactive species, portable and low cost instrumentation.

1.2.1.4 Faradaic and Non-Faradaic Processes

The current response obtained in controlled–potential experiments is as a result of the analyte species that is oxidized or reduced at the electrode–solution interface. This current response is deduced from the transfer of electrons during the redox process of the target analyte as shown in Equation 1.2:

$$\mathrm{Ox} + \mathrm{ne}^{-} \rightleftharpoons \mathrm{Red} \qquad 1.2$$

where Ox and Red represent the oxidised and reduced forms of the analyte, respectively, while n is the number of electrons transferred. The current that arises from the oxidation or reduction of the analyte species is called the Faradaic current. For a thermodynamically controlled reversible process the applied potential (E) of the electrode is given by the well known Nernst equation, Equation 1.3:

$$E = E^{\circ} + \frac{2.303RT}{nF}\log\frac{C_{ox}}{C_{red}} \qquad 1.3$$

where E^{o} = standard potential of the redox couple; R = universal gas constant; T = temperature (K); n = number of electrons transferred; F = Faraday’s constant; C_{ox} = Concentration of the oxidized species; C_{red} = Concentration of the reduced species.

Non Faradaic currents are a result of those processes that do not involve the transfer of electrons across the electrode–solution interface and they stem from the electrical capacitance present at the interface. The capacitance (C) of the electrical double layer can be calculated using Equation 1.4.

$$C = \frac{q}{E} \qquad 1.4$$

where q and E represent charge and potential respectively.

1.2.1.5 The Electrochemical Cell

All current-measuring (voltammetric / amperometric) techniques make use of a three-electrode electrochemical cell (Fig. 1.3) [4-6].

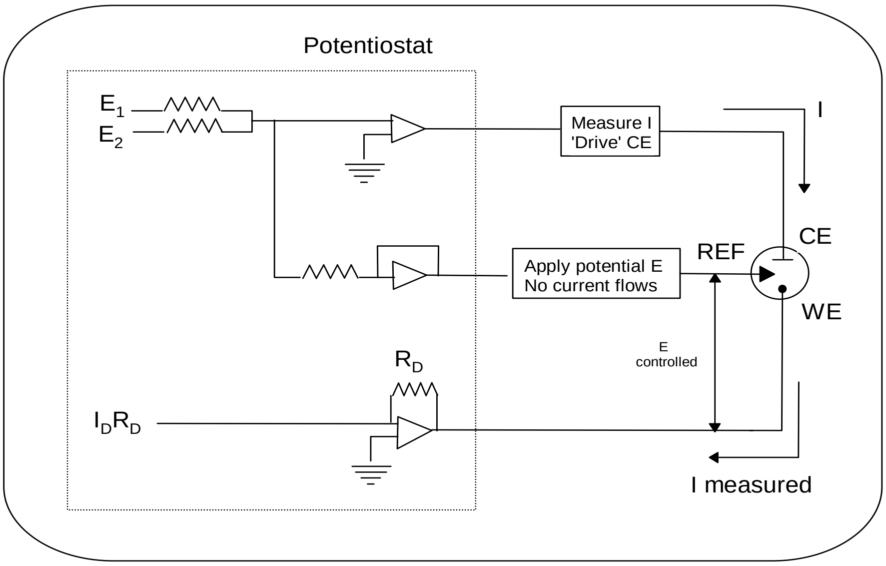

Figure 1.3: Graphical representation of a conventional three-electrode cell [5].

The surface of the working electrode, W.E., is the platform of the electrochemical reaction being studied. R.E. is the reference electrode, while the counter electrode, C.E., completes the electric circuit. The best reference electrode is one whose potential does not shift from equilibrium (i.e. non polarisable). In order to minimize the potential shift, a reference electrode with very large surface area is often used [1]. Potentiostats based on operational amplifiers are often used in the complete elimination of reference electrode polarisation. As shown in Figure 1.1 the potentiostat maintains the potential difference, ∆E, between the R.E. and W.E. and supplies the current, i, needed for affecting the changes occurring at W. E.

There are numerous reference electrodes employed in electroanalytical experiments, but the most common being the silver|silver chloride (Ag|AgCl, sat'd KCl) electrode. It is a piece of silver wire anodized with silver chloride which is immersed in potassium chloride or sodium chloride solution and encased in a glass tube. The electrode is protected from the bulk of the solution by a non-selective salt-bridge [7]. Platinum rods, wire, loops, gauze or foil are consistently used as counter electrodes. Commonly used working electrodes include mercury, carbon and inert materials such as platinum or gold.

1.2.1.6 Mass Transport Processes

The fundamental movement of charged or neutral species in an electrochemical cell to the electrode surface is facilitated by three processes namely: diffusion, migration or convection [2,3] as illustrated in Figure 1.4.

Diffusion is mass transport resulting from the spontaneous movement of analyte species from regions of high concentrations to lower ones, with the aim of minimizing concentration differences. A concentration gradient develops if an electrochemical reaction depletes (or produces) some species at the electrode surface. To minimize the concentration difference an electroactive species will diffuse from the bulk solution to the electrode surface (or from the electrode surface into the bulk solution.

Migration refers to movement of a charged particle in a potential field. In most voltammetric experiments, migration is undesirable but can be eliminated by the addition of a large excess of supporting electrolyte. Inert anions and cations (i.e., electrochemically inert – not oxidized or reduced) that are formed from dissociation of the supporting electrolyte now function as the migration current carriers and also increase the conductivity of the solution [1].

Finally ***convection*** is a mass transport achieved by some form of external mechanical energy acting on the solution or the electrode such as stirring the solution, solution flow or rotation and/or vibration of the electrode.

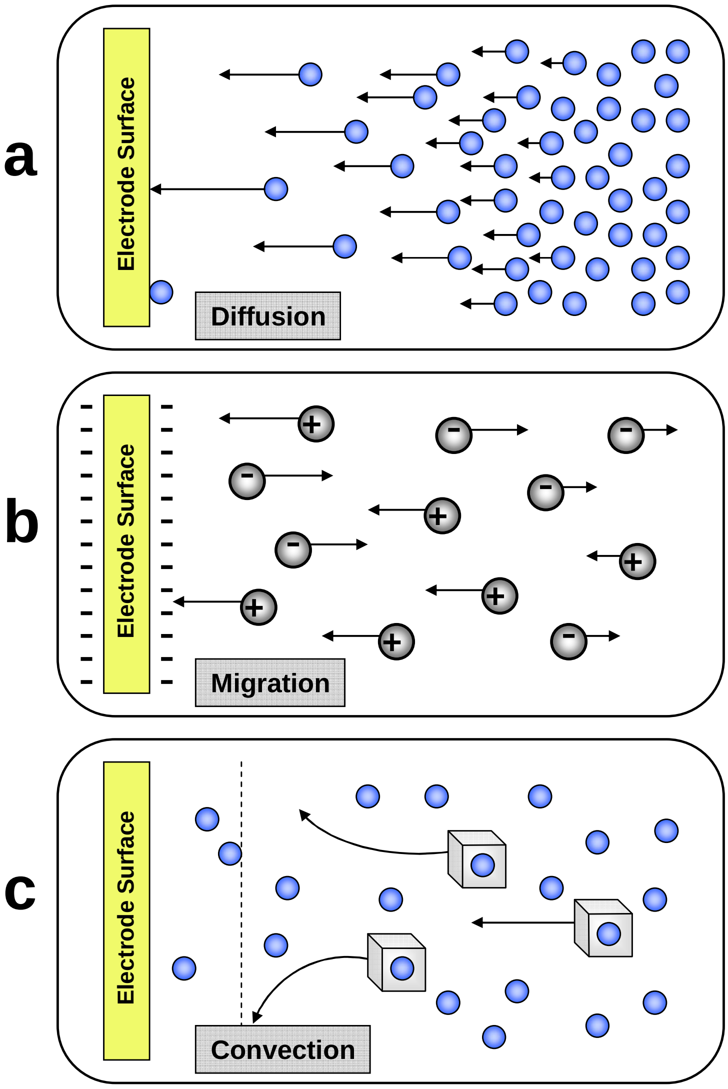

Figure 1.4: Schematic representation of the three mass transport modes viz. (a) Diffusion, (b) Migration and (c) Convection [2].

1.2.2 Voltammetry

Voltammetry is a branch of electroanalytical techniques and it is often used in industrial processes to obtain information about the analyte species by varying the potential and measuring the current.

1.2.2.1 Types of Voltammetry

1.2.2.1.1 Cyclic Voltammetry

Cyclic voltammetry (CV) depicted in Figure 1.5 is the most extensively used electrochemical technique and is used to study electrochemical reactions as well as to provide information on the reversibility and kinetics of such reactions [5,8]. During a cyclic voltammetry experiment, the potential of an electrode is scanned linearly from an initial potential to a final potential and then back to the initial potential. The potential at which the peak current occurs is known as the peak potential (E_p) where the redox species has been depleted at the electrode surface and the current is diffusion limited. The magnitude of the Faradaic current (I_{pa} - anodic peak current) or (I_{pc} - cathodic peak current), gives an indication of the rate at which electrons are being transferred between the redox species and the electrode. Cyclic voltammetric processes could be reversible, quasi-reversible and irreversible.

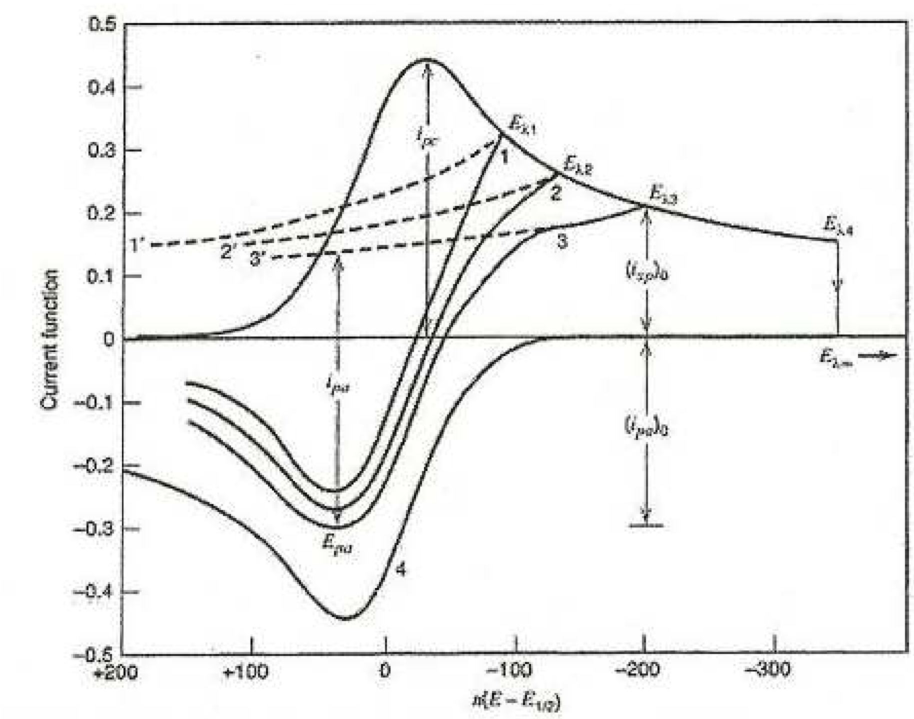

Figure 1.5: Typical cyclic voltammogram for a reversible process [3].

Reversible Process

A reversible process is one in which the electron transfer process is rapid, and the electroactive oxidised (or reduced) species in the forward scan is in equilibrium with the electroactive reduced (oxidised) species in the reverse scan (Eq. 1.5).

$$\mathrm{Red} \rightleftharpoons \mathrm{Ox} + ne^- \tag{1.5}$$

Figure 1.5 shows a typical CV for a reversible process. The electroactive species are stable and so the magnitudes of I_{pc} and I_{pa}

are equal and proportional to the concentrations of the active species. ΔE_p ($E_{pa} - E_{pc}$) should be independent of the scan rate (ν) but in practice ΔE_p increases slightly with increasing ν, this is due to the solution resistance (R_S) between the reference and working electrodes [9,10]. Theoretically, the potential difference between the oxidation and reduction peaks is 59 mV for one-electron reversible redox reactions. However, in practice, ΔE_p is sometimes found in the 60-100 mV range.

Reversibility is a direct and straight forward means of probing the stability of an electroactive species. An unstable species reacts as it is formed and hence produces no current wave in the reverse scan whereas a stable species remains in the vicinity of the electrodes surface and produces a current wave of opposite polarity to the forward scan. Larger differences or asymmetric reduction and oxidation peaks are an indication of irreversible reactions. Irreversibility is a result of slow exchange between the redox species and the working electrode [5]. At 25°C, the peak current is given by the Randles-Ševčík equation [2,3]:

$$i_p = \left(2.69\times10^5\right)n^{3/2}AC\left(D\nu\right)^{1/2} \qquad 1.6$$

where, i_p = peak current (A); n = number of electrons transferred; A = electrode area (cm^2); C = concentration (mol cm^{-3}); D = diffusion coefficient (cm^2 s^{-1}) and ν = scan rate (V s^{-1}). These parameters make CV most suitable for characterization and mechanistic studies of redox reactions at electrodes.

A linear plot of i_p vs. $\nu^{1/2}$ indicates that the currents are controlledby planar diffusion to the electrode surface [9]. The ratio of anodic to cathodic currents i_{pa} / i_{pc} is equal for a totally reversible process and deviation from this is indicative of a chemical reaction involving either one or both of the redox species. The potential where the current is half of its limiting value is known as the half-wave potential $E_{1/2}$ (also called formal potential or equilibrium potential, $E°'$) which is the average of the two peak potentials, represented by Equation 1.7.

$$E_{1/2}(or E^{\circ'}) = \frac{E_{pa} + E_{pc}}{2} \qquad 1.7$$

where E_{pa} and E_{pc} are the anodic and cathodic peak potentials, respectively. The separation between two peak potentials, ΔE_p for a reversible couple is given by Equation 1.8 and can be used to obtain the number of electrons transferred.

$$\Delta E = E_{pa} - E_{pc} = 2.303\frac{RT}{nF} \qquad 1.8$$

ΔE_p is independent of the scan rate, and at 25 °C Equation 1.8 can be simplified to Equation 1.9:

$$\Delta E_p = 2.303\frac{RT}{nF} = \frac{0.059V}{n} \qquad 1.9$$

At appropriate conditions (i.e. at 25 °C, first cycle voltammogram) the standard rate constant (*k*) for the heterogeneous electron transfer process can be estimated [1,11].

Irreversible Process

For an irreversible process, only forward oxidation (reduction) peak is observed but at times with a weak reverse reduction (oxidation) peak as a result of slow electron exchange or slow chemical reactions at the electrode surface [7]. The peak current, i_p for irreversible process is given by Equation 1.10:

$$i_p = \left(2.99\times10^5\right)n\left[(1-\alpha)n\right]^{1/2} Ac\left(D\nu\right)^{1/2} \qquad 1.10$$

where α is the coefficient of electron transfer, the rest of the symbols are defined above in Equation 1.3. For a totally irreversible system, ΔE_p is calculated from Equation 1.11:

$$\Delta E_p = E^{o'} - \frac{RT}{\alpha nF}\left[0.78 - \ln\frac{k}{D^{1/2}}\ln\left(\frac{\alpha nF}{RT}\right)^{1/2}\right] \qquad 1.11$$

where all symbols are defined above. At 25 °C, E_p and $E_{1/2}$ differ by $0.048/\alpha n$.

Quasi-Reversible Process

Unlike the reversible process in which the current is purely mass-transport controlled, currents due to quasi-reversible process are controlled by a mixture of mass transport and charge transfer kinetics [2,12]. The process occurs when the relative rate of electron transfer with respect to that of mass transport is insufficient to maintain Nernst equilibrium at the electrode surface. For quasi-reversible process, i_p increases with $\nu^{1/2}$ but not in a linear relationship and $\Delta E_p > 0.059/n$ [3]. The slight differences in three cyclic voltammetric processes are summarized in Table 1.1.

Table 1.1: The diagnostic criteria for reversible, irreversible and quasi-reversible cyclic voltammetric processes [3,7,12]

Parameter	**Cyclic Voltammetry Process**		
	Reversible	*Irreversible*	*Quasi-reversible*
E_p	Independent of ν	Shifts cathodically by 30/αn mV for a 10-fold increase in V	Shifts with ν
E_{pc} - E_{pa}	~ 59/n mV at 25°C and independent of ν	_	May approach 60/n mV at low ν but increases as ν increases
I_p / $\nu^{1/2}$	Constant	Constant	Virtually independent of ν
I_{pa} / i_{pc}	Equals 1 and independent of ν	No current on the reverse side	Equals 1 only for α = 0.5

1.2.2.1.2 Square Wave Voltammetry

In square wave polarographs the base-current can be suppressed by using alternating voltage of square-wave shape, where the base-current decays more rapidly than the Faradaic current after the application of a voltage-pulse to the electrode. Therefore, a measurement of the current a short time before each new pulse leads to elimination of the base-current from the recorded polarogram. This principle was first used in the square-wave polarograph of Barker and Jenkins [13]. Janet G. Osteryoung used this concept to develop the differential electrochemical technique, Square Wave Voltammetry (SWV) [14]. It depends on excitation functions that overlay the features of a large amplitude square wave modulation and a single staircase waveform [15]. Throughout any given square wave cycle, the current is sampled at the end of the forward and reverse scans and the difference between the forward (i_f) and reverse current (i_r), are plotted against the average potential of each waveform cycle. In this technique, the peak potential occurs at the $E_{1/2}$ of the redox couple because the current function is symmetrical around the half-wave potential [15]. The scan rate of a square wave voltammetry experiment is given by the Equation 1.12:

$$\nu = f.\Delta E_s \qquad 1.12$$

where f is the square wave frequency (Hz) and ΔE_s is the potential step size. Major advantages of this powerful electrochemical technique include its capacity to use of faster scan rates compared to conventional differential pulse voltammetry, its ability to reject capacitive charging currents and its fantastic sensitivity.

1.2.2.1.3 Chronoamperometry

Chronoamperometry (CA) is an electrochemical technique that is a simple short-lived amperometric method where the current is recorded as a function of time as a result of the potential being stepped. This uncomplicated potential step wave form (Fig. 1.6) monitors the current response following the working electrode potential being stepped from an initial potential at which the oxidized (reduced) species is stable in solution, to the first step potential where a redox reaction occurs forming the reduced (oxidized) species and it is held at this value for the duration of the first step time in a single potential experiment. In a double potential step experiment, the potential is stepped twice. First for the period mentioned above and thereafter that stepped to a second step potential where it is held for the duration of the second step time.

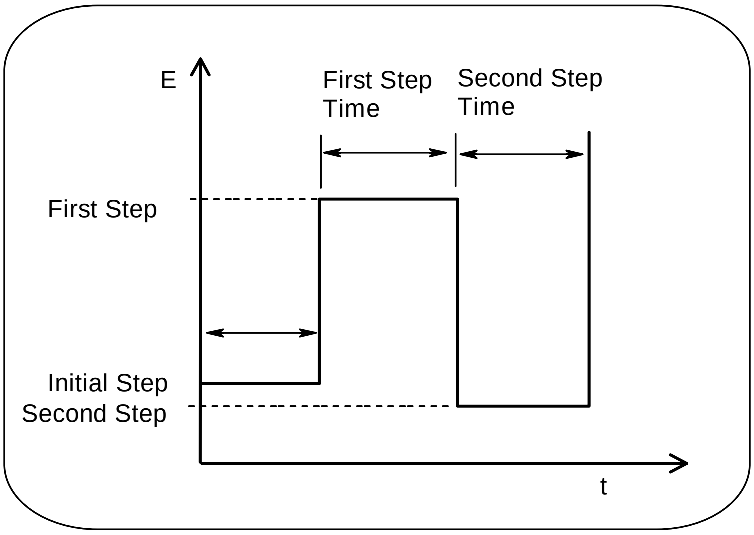

Figure 1.6: Simple potential wave form depicting chronoamperometry.

The analysis of chronoamperometry (CA) data is based on the Cottrell equation, 1.13 [16-18]. A plot of i versus $t^{-1/2}$ is often referred to as the Cottrell plot which defines the current-time dependence for linear diffusion control and can be used to calculate the diffusion coefficient (D) resulting from the slope of the plot.

$$i = nFACD^{1/2}\pi^{-1/2}t^{-1/2} \qquad 1.13$$

where n = number of electrons transferred /molecule; F = Faraday's constant (96 485 C mol^{-1}); A = electrode area (cm^2); D = diffusion coefficient (cm^2 s^{-1}); C = concentration (mol cm^{-3}) and t = time (s)At intermediate times of chronoamperometric measurements the catalytic rate constant (k) can be determination using the established Equation 1.14 [3, 16-18]:

$$\frac{I_{cat}}{I_L} = \pi^{1/2}\left(kC_o t\right)^{1/2} \qquad 1.14$$

where I_{cat} and I_L are the currents of the electrode in the presence and absence of the analytes, respectively; k and t are the catalytic rate constant (M^{-1} s^{-1}) and time elapsed (s), respectively; and C_o is the bulk concentration of analytes. The catalytic rate constant can be determined from the slope of the plot of I_{cat} / I_L vs. $t^{1/2}$.

1.2.2.1.4 Rotating Disk Electrode

A rotating disk electrode (RDE) is a hydrodynamic working electrode that is used in a three electrode system [3]. This technique is usually employed in electrochemical studies when investigating redox related mechanistic reactions. The conductive disk or working electrode is made of glassy carbon or a noble metal which is embedded in an inert non-conductive polymer or resin. In this technique the working electrode, controlled by the attached electric motor, actually rotates, and in so doing provides an influx of the analyte species at the electrode surface. The disk’s rotation is often described in terms of angular velocity. As it turns it pulls the solution closest to its surface (hydrodynamic boundary layer) with, creating a whirlpool effect thus the solution from the centre of the electrode is displaced as a result of centrifugal force. Solution from the bulk now flows up, perpendicular to the electrode, to replace the boundary solution. The sum result is a laminar flow across and towards the electrode surface. The rate of the rotating disk controls the solution flow which in turn controls the steady-state current. This method is different to unstirred techniques where the steady-state current is controlled by diffusion. In this work I used linear sweep voltammetry at various rotation speeds to investigate the electron transfer behaviour.

The analysis of RDE data is based on the Equation 1.15: A plot of limiting current (I_L) vs. $\omega^{1/2}$ which is often referred to as the Koutecky-Levich plot and can be used to calculate the catalytic rate constant, k_{ch}, resulting from the slope of the plot.

$$\frac{1}{i_{\lim}} = \frac{1}{i_k} + \frac{1}{i_{lev}} = \frac{1}{(nFAk_{ch}\Gamma C)} + \frac{1}{(0.620nFAcD^{2/3}\gamma^{-1/6}\omega^{1/2})} \qquad 1.15$$

where i_{lim}, i_k, i_{lev} are the measured current, kinetic and diffusion-limited currents, respectively, n is the number of electrons transferred which is 2 for epinephrine electrooxidation, k_{ch} is the catalytic rate constant ($mol^{-1}\ cm^3\ s^{-1}$) obtained from the intercepts of the regression lines, F is the Faraday constant (96 485 C mol^{-1}), A is the electrode surface area which is 0.1963 cm^2, ω is the rotating speed (rps), Γ (mol cm^{-2}) is the redox active species (DMAET-SWCNT-PABS) concentration on electrode surface, C is the bulk concentration of analyte (mol cm^{-3}), D is the diffusion coefficient (cm s^{-1}) of epinephrine and γ is the kinematic viscosity of the solution.

1.2.2.1.5 Linear Sweep Voltammetry

Linear sweep voltammetry (LSV) is a voltammetric method that measures the current at the working electrode while the potential between the working and a reference electrode is linearly swept in time. A measure of the current signal is denoted by a peak or trough that is formed at the potential where the species begins to be oxidized or reduced. Linear sweep voltammetry is a general term applied to any voltammetric method in which the potential applied to the working electrode is varied linearly in time. These methods would include polarography, cyclic voltammetry, and rotating disk voltammetry. LSV is similar to CV except that the potential range is scanned starting at the initial potential and ending at the final potential whereas in CV the direction of the potential scan is reversed at the end of the forward scan, and the potential range is scanned again in the reverse direction. In the case of CV the potential changes as a linear function of time and the rate of change of potential with time is referred to as the scan rate.

1.2.2.2 Electrocatalysis Using Voltammetry

Electrocatalysis using voltammetric techniques is characterized by current enhancement and/or a potential shift to lower values in the case of CV and SWV. Scheme 1.1 shows the basic mechanisms through which electrocatalytic reactions operate at electrodes modified with a catalyst (such as SWCNT-PABS, MPCAuNP or MPc as studied in this project).

The catalyst is first oxidized, which then interacts with the analyte leading to the formation of the oxidized analyte and regeneration of the catalyst [19,20]. Electrocatalysis amplifies the detection signal of an analyte resulting in faster electrode reactions at a lower potential in comparison to the bare (unmodified) electrode. Lowering of detection potentials minimizes interferences from co-existing electroactive species. Chemically modifying the electrodes improves their electrocatalytic current necessary for sensitive detection of target analytes using cyclic voltammetry, square wave voltammetry or chronoamperometry.

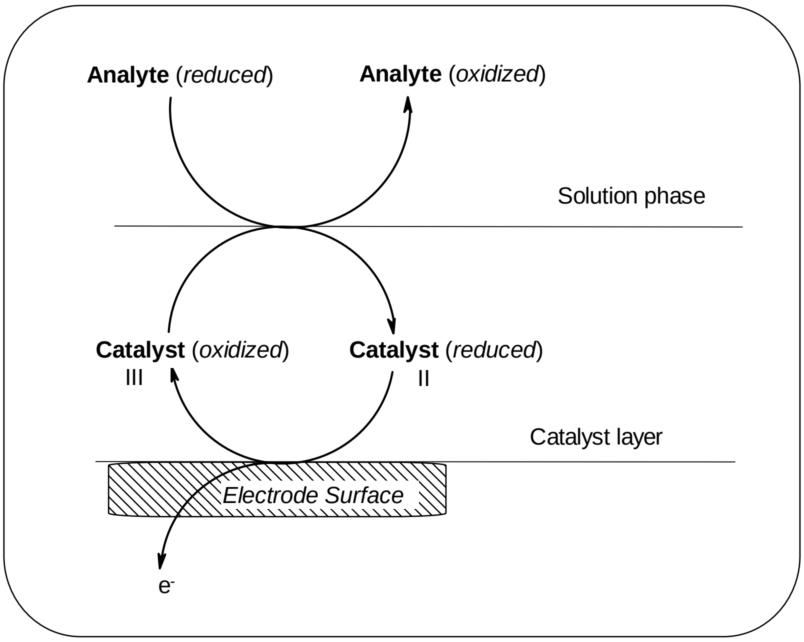

Scheme 1.1: Generalized schematic representation of electrocatalysis at an electrode modified with a catalyst.

1.2.3 Electrochemical Impedance Spectroscopy

Electrochemical Impedance Spectroscopy (EIS) is a very versatile electrochemical tool used to investigate the electrochemical properties of systems and their interfaces with conductive electrodes [21]. It is an effective technique for interrogating the kinetics at interfaces and distinguishing between the various mechanisms that govern charge transfer [21-23]. EIS can be used in various applications, however, this work focuses on its ability to characterize thin film formation and hence determine its electron transport properties.

Basics of impedance spectroscopy

The principle of impedance stems from the alternating current theory that defines the response to an alternating current or voltage as a function of frequency [21]. Impedance is the opposition to the flow of alternating current in a complex electrical system and is measured by applying a sinusoidal potential, V (t), of small amplitude to an electrochemical cell and measuring resultant sinusoidal current, I (t), through the cell [21,24]. The applied sinusoidal potential and resulting sinusoidal current are represented as a function of time. These measurements are done over a suitable frequency range and the results can be related to the physical and chemical properties of the material [21,25]. The relationship is shown in Equation 1.16:

$$Z = \frac{V(t)}{I(t)} \qquad 1.16$$

where V (t) is the sinusoidal applied voltage at time t, $V(t) = V_o \sin \omega t$ where V_o is the maximum potential amplitude, ω is the radial frequency (in rad s^{-1}) and can be related to frequency f (Hz) as $\omega = 2\pi f$. However, the current response is only sinusoidal if the voltage amplitude is small relative to 59 mV, and centered at the OCP. At the same frequency as the applied sinusoidal potential the current response I(t) is also sinusoidal but with a shift in phase, $I(t) = I_o \sin(\omega t + \theta)$, where I_o is the maximum current applied and θ represents the phase shift by which the voltage lags the current [3,21] as depicted in Figure 1.7 (a). The impedance is a vector quantity with magnitude and direction. The magnitude of impedance is Z (V / I) and the direction is represented as a phase angle, θ as shown in Figure 1.7 (b). Impedance can be represented by Equation 1.17:

$$Z = Z' + jZ'' = Z_{real} + jZ_{imaginary} \qquad 1.17$$

where Z' and Z'' are the real and imaginary parts of the impedance, respectively and j is a complex number [24].

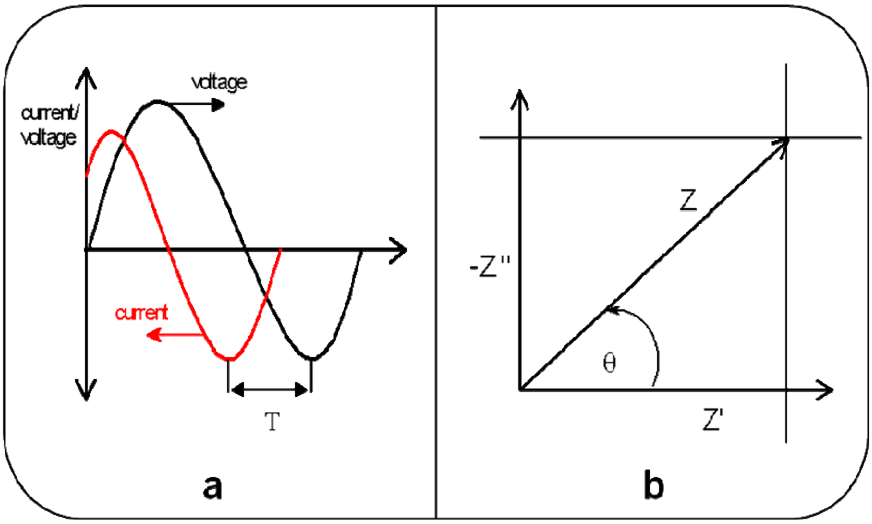

Figure 1.7: (a) Applied sinusoidal voltage and resulting sinusoidal current response. (b) Vector representation of real Z' and imaginary Z'' parts of impedance (Z) [21,24].

Data representation of EIS

Impedance data can be analysed using equivalent circuits i.e. circuits that "fit" the impedance data with the least possible error percentage. The impedance data were fitted to an equivalent circuit using the FRA software package for complex non-linear least squares calculations based on the EQUIVCRT programme. Within the circuit, simple electric elements such as resistors and capacitors, measuring resistance and capacitance respectively, are connected to model the electrochemical process [21,24]. The resistance in the circuit is an indication of the electrical conductivity of the electrolyte and the constant phase element (CPE) results from the charge which is in excess at the electrode-electrolyte interface. Ideal Randles equivalent circuit involves double layer (C_{dl}) as shown in Figure 1.8 (a), while modified Randles circuit uses CPE as illustrated in Figure 1.8 (b). CPE is for real, practical situations. CPE may occur as a result of several factors [21], including (i) the nature of the electrode (e.g., roughness and polycrystallinity), (ii) distribution of the relaxation times due to heterogeneities existing at the electrode/electrolyte interface, (iii) porosity and (iv) dynamic disorder associated with diffusion. The impedance of CPE is given as [21]:

$$Z_{CPE} = \frac{1}{[Q(j\omega)^n]} \qquad 1.18$$

where Q is the frequency-independent constant relating to the surface electroactive properties, ω is the radial frequency, the exponent n arises from the slope of the bode plot; log Z vs. log f (and has values $-1 \leq n \leq 1$). If $n = 0$, the CPE behaves as a pure resistor; $n = 1$, CPE behaves as a pure capacitor, $n = -1$ CPE behaves as an inductor; while $n = 0.5$ corresponds to Warburg impedance (Z_w) which is associated with the domain of mass transport control arising from the diffusion of ions to and from the electrode|solution interface.

The Randles equivalent circuit may be employed to "fit" the electrochemical impedance data depending on the nature of the impedance data. There are numerous circuits that can be assembled in order to provide the most accurate "fit". An indication of the correct circuit that may be used to fit the data is given by the graphical representation of the impedance data referred to as the Nyquist plot. The Nyquist plot ($Z_{\text{imaginary}}$ vs. Z_{real}) shown in Figure 1.9 a displays a characteristic semi-circle at high frequencies and a straight line at low frequencies, corresponding to kinetic and diffusion processes, respectively, where The described spectra is generally fitted using the Randles equivalent circuit of mixed kinetic and diffusion control, where the resistance of the electrolyte and electrode contacts, R_S is connected in series to the parallel combination of charge-transfer resistance R_{CT} (domain of kinetic control) and CPE. The resistance to charge-transfer is proportionally related to the diameter of the semi-circle of the nyquist plot. In some systems the reaction rate might be controlled by transport phenomenon and this effect needs to be taken into consideration, the measured impedance can be explained by the component that depends on the conditions of the transport or diffusion of ions to the electrode interface from the bulk of the electrolyte [21,24]. This component is known as the Warburg impedance (Z_W) (domain of mass transport control) and is connected in series to the charge transfer resistance. In this work, the Randles equivalent circuit was predominantly used to fit the electrochemical data.

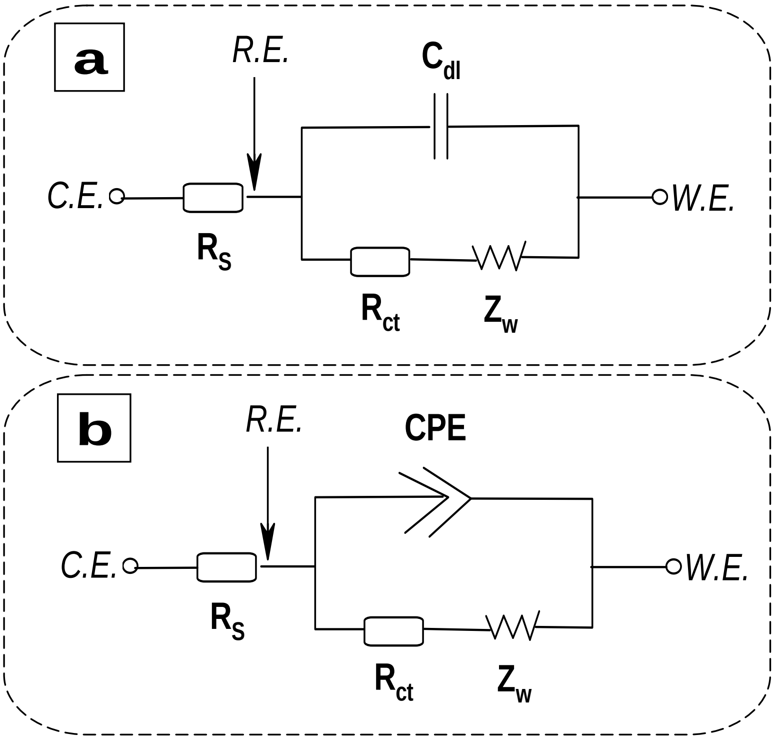

Figure 1.8: Modified Randles equivalent circuit representing the electrochemical system in (a) Ideal situation and (b) Real, practical situation.

Impedance data can also be graphically represented by bode plots shown in Figure 1.9 (b) [21,25]. From the plot of phase angle (θ) vs. logarithm of the frequency (log. f), the peak height represented the capacitive nature of the electrode surface and the relaxation process of the electrode|solution interface is indicated by the phase angle and frequency values respectively. A phase angle of 90° implies the material on the electrode surface displays pure capacitance, whereas a value of less than 90° indicates a more pseudo-capacitive behaviour [24]. As mentioned above, the capacitive nature of the electrode surface is also attained from the value of the slope from the plot of the log. |Z| vs. log f (Fig. 1.9 b).

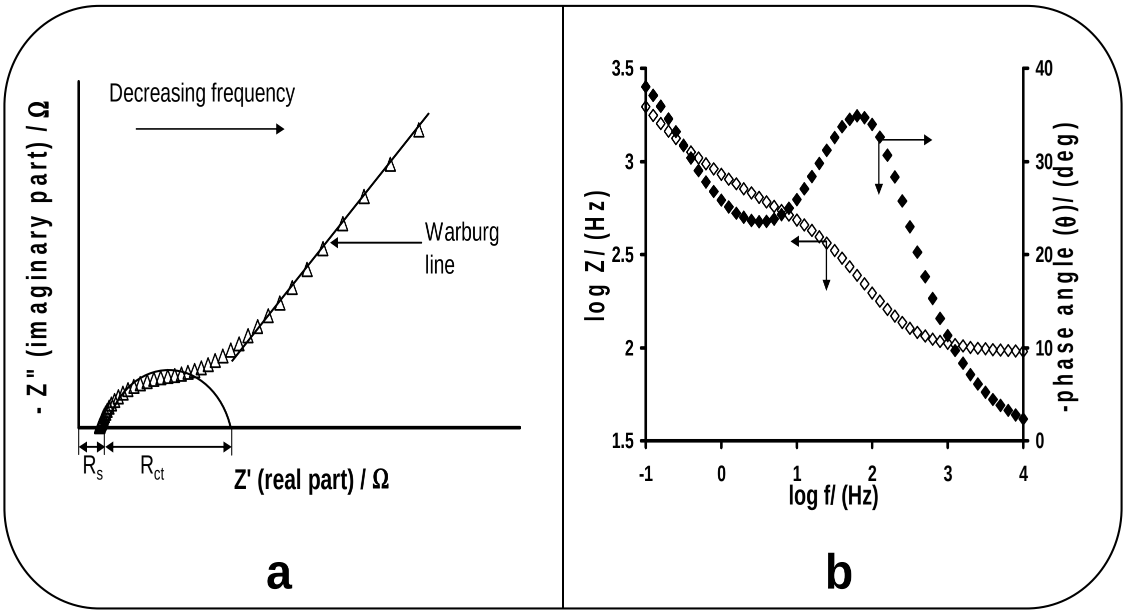

Figure 1.9: Nyquist plot (a) and Corresponding bode plot (b) for the randles equivalent circuit.

Electrochemical impedance spectroscopy offers several advantages over other techniques, these include: (i) the capacity of the system to remain at equilibrium due to the use of low amplitude-sinusoidal voltage (~ 5 mV), (ii) the ability to obtain accurate, reproducible measurements, (iii) the capability of this technique to adapt to various applications, (iv) characterize interfacial properties in the absence of redox reactions and (v) rapid acquisition of data such as ohmic resistance, capacitance, film conductivity, as well as charge or electron transfer at the electrode-film interface.

An electrode-film interface is a result of the electrode modification with electron transfer mediators such as carbon nanotubes or redox active nanomaterials in order to overcome the sluggish electron transfer behaviour at the bare electrode. The following section describes a few regularly used electrode modification techniques.

1.3 Modified Electrodes

According to International Union of Pure and Applied Chemistry (IUPAC) [26], a chemically modified electrode (CME) can be defined as "an electrode made of a conducting or semi-conducting material that is coated with a film of a chemical modifier and that by means of Faradaic (charge transfer) reactions or interfacial potential differences (no net charge transfer) exhibits chemical, electrochemical, and/or optical properties of a film." In other words, if a specific material is attached to the surface of an electrode then that material imparts on the electrode some chemical, electrochemical or desirable properties not available at the unmodified electrode [27-29]. However, the material first needs to be immobilized onto the surface of the electrode.

1.3.1 General Methods of Modifying Electrode Surfaces

There are numerous techniques that may be used to modify electrode surfaces. A few are listed below.

Covalent Bonding

This method employs a linking agent (e.g. an organosilane) to covalently attach one of several monomolecular layers of the chemical modifier to the electrode surface [30-31].

Drop-dry Coating (or solvent evaporation)

A few drops of the polymer, modifier or catalyst solution are dropped onto the electrode surface and left to stand to allow the solvent to dry out [32].

Dip-dry Coating

The electrode is immersed in a solution of the polymer, modifier or catalyst for a period sufficient for spontaneous film formation to occur by adsorption. The electrode is then removed from solution and the solvent is allowed to dry out [33].

Composite

The composite electrode is prepared by a simple impregnation of the bulk electrode material with a chemical modifier such as an MPc catalyst. A good example is the popular carbon paste electrode [34].

Spin-Coating (or spin-casting)

This method involves evaporating a drop of polymer, modifier or catalyst solution from an electrode surface by using centrifugal force at high-speed rotations. For example, oxide xerogel film electrodes prepared by spin-coating a viscous gel on an indium tin oxide substrate [35].

Electrodeposition

In this method, the electrode surface is immersed in a concentrated solution (~10^{-3} mol L^{-1}) of the polymer, modifier or catalyst followed by repetitive voltammetric scans. The first and second scans are similar, subsequent scans decrease with the peak current. For example, electrochemical deposition of poly(*o*-toluidine) on activated carbon fabric [36].

Electropolymerization

In this technique the electrode is immersed in a polymer, modifier or catalyst solution and layers of the electropolymerized material builds on the electrode surface. Generally, the peak current increases with each voltammetric scan such that there is a noticeable difference between the first and final scans indicating the presence of the polymerized material. For example, electropolymerization of aniline on polyaniline modified platinum electrodes [37].

Langmuir-Blodgett Technique

This technique involves transferring the ordered monolayer or multilayer film formed at the air/water interface onto the electrode surface [38].

Chemisorption

In this method, the chemical film is strongly and ideally irreversibly adsorbed (chemisorbed) onto the electrode surface [30]. Electrode modification using self assembled monolayer falls into this category.

1.3.2 Self-Assembly

Smart immobilisation of ultrathin solid films of nanomaterials on solid surface has continued to attract major research interests because of the potential to open up a wide range of diverse novel technological and engineering applications. In this regard, immobilisation of materials on electrode surfaces, using the conventional self-assembly strategy [39] to form molecular monolayers and its related layer-by-layer self-assembly [40] to form molecular multi-layers have continued to receive considerable attention. Self-assembly method is advantageous because of its simplicity and control of the order of materials build-up which might allow synergic relationship between the materials towards specific purposes.

1.3.2.1 Self-Assembled Monolayer-Modified Electrodes

The self-assembled monolayer (SAM) may be described as the ordered arrangement of spontaneously adsorbed molecules (such as thiol species) from solution directly onto the surface of an appropriate substrate (such as gold) resulting in the formation of an ultrathin film [1,41]. In 1946, four decades after Langmuir [42] introduced the concept of monolayers, Zisman [43] demonstrated the self-assembly of alkylamine monolayers onto a platinum substrate. Since then a number of adsorbate/substrate SAM forming combinations have been found that are able to form SAMs e.g., alkyltrichlorosilanes on glass [44] and fatty acids on metal oxides [45]. In 1983, Allara and Nuzzo [46] showed the adsorption of sulphur-containing compounds onto gold surfaces. However, it was only after the numerous articles published in 1987 and 1988 that there was an influx of thiol based SAM research [47-50]. Since then the fabrication of ultrathin, well-ordered self-assembled monolayer films of thiol-derived organic molecules on gold substrates have been a major research interest due to the potential ability of such ultrathin films to be used as scaffolds in a plethora of nanotechnological applications and fundamental studies including the immobilization of biomolecules (e.g., proteins, DNA) and redox-active functional materials for catalysis and sensing. For example, several potential applications of carbon nanotubes mean that some of their future applications in catalysis, sensing and electronics will require their integration on solid substrates as ultrathin nano-scaled molecular films.

Sulphur containing compounds (eg. thiols) have a high affinity for gold and are used in the self assembly formation of the base monolayer on gold surfaces. Cysteamine is one such example which also allows for the covalent attachment of other species. In 1997, Caruso *et al.* [51] introduced a 2-dimethylaminoethanethiol (DMAET) SAM as a platform for integrating DNA on gold surfaces. Since then, no work has been reported on this important SAM. This motivated me to use this innovative SAM as a potential base monolayer for forming multilayer films. However, successful future applications of DMAET SAM is dependent on thorough understanding of the state of the amino head group from which further surface functionality can be derived. Therefore, in this work, I have used cyclic voltammetry and electrochemical impedance spectroscopy to probe the behaviour of the $-NH^+(CH_3)_2$ head group of DMAET SAM in solutions containing outer-sphere redox probe ($K_4Fe(CN)_6$ / $K_3Fe(CN)_6$), different electrolytes and epinephrine.

From an electrochemistry point of view, the chemisorption of thiolates on gold depicted in Figure 1.10 is regarded [1] as the most important class of SAMs. The nature and the formation of the bond between gold surface and the thiol has been a subject of much interest [1,52-55] but it is often recognised that the gold-thiolate bond results from cleavage of the S-H bond. Gold substrates are preferred in thiol

SAMs because of the strong interaction between gold and sulphur that allows the formation of monolayers in the presence of many other functional groups [54]. Generally, the central feature of all SAMs is the strong interaction between the functional group of the adsorbate and the bare substrate as well as the van der Waals interactions among the adsorbed molecules [1].

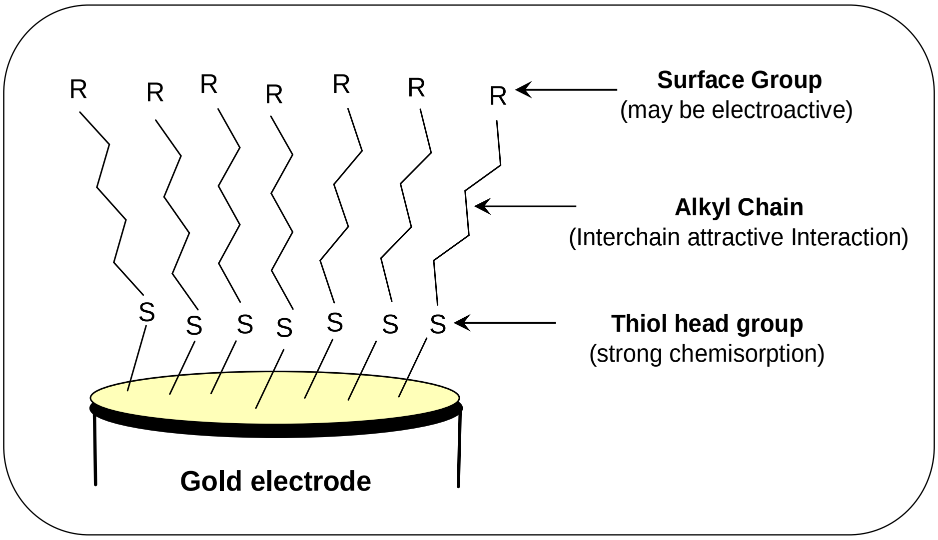

Figure 1.10: Representation of a thiolate on gold SAM.

The self-assembling technique offers several advantages over other film formation techniques which include:

(a) Spontaneous adsorption onto the electrode surface resulting in the formation of a thermodynamically equilibrated final film structure.

(b) The SAM film does not readily undergoing desorption as a result of the sulphur-gold bond.

(c) The adsorbate does not have to be compatible with water like in the case of the Langmuir-Blodgett technique.

(d) The cost effectiveness of the fabrication process because it does not require expensive equipment.

(e) The orientation of the film (lying flat or standing perpendicular to the substrate) can be controlled, for example the formation of mixed monolayer.

Additional molecular material may be added onto the primary monolayer by means of the layer-by-layer technique.

1.3.2.2 Layer-by-layer Self Assembly

One of the elegant means of forming ultrathin films on solid substrates is the self-assembly used in forming molecular monolayers, and the layer-by-layer (LBL) self-assembly for forming molecular multi-layers. LBL has recently been elegantly reviewed by Zhang *et al.* [56]. LBL, first discovered in 1966 by Iler [57] and re-discovered in 1991 by Decher and Hong [58,59] may simply be described as controlled coordination or stepwise self-assembly strategy based on the alternating adsorption of materials containing complementary charged or functional groups to form integrated, well-organized arrays of ultrathin superstructure films on solid surfaces [56] that are often less than 1 μm [60,61], on solid surfaces. This strategy could provide a powerful bottom-up approach for the construction of nano-scaled 3D architectures with various properties. Indeed, the simplicity and versatility of this technique makes it admirable for producing high quality and consistent films.

After the introduction of the LBL technique based on physical adsorption driven by ionic attraction, other LBL methods emerged. Some of which were based on hydrogen bonds, step-by-step reactions, sol–gel processes, molecular recognition, charge-transfer, stepwise stereocomplex assembly and electrochemistry [56]. This work concentrates on the LBL method that uses electrostatic interaction as the main driving force. The basic principle in the assembly is "charge reversal", where oppositely charged material referred to as bilayers are successively adsorbed. Each bilayer is approximately 1-100 nm thick [62] and can be tailored by adjusting the pH [63], counter ion [64], ionic strength [65], chemistry [66], molecular weight [67] and temperature [68]. The original construction of these multilayer films involved the use of polyelectrolytes, and thereafter extended to conjugated polymers [69-71], nanomaterials [72,73], dye and drug crystals [74], organic latex particles [75], inorganic particles [76], protein [77], biological cells [78], DNA [79], antigen-antibody pairs [80], CNTs [81] metallophthalocyanines [82] and monolayer-protected-clusters of gold

[83]. This LBL technique produces high quality and consistent films that have a few advantages over other multilayer fabrication processes.

(a) The fabrication of multilayers is a simple method that does not require the use of complicated instruments.

(b) The deposition times and material used during the process are user controlled.

(c) The prospect of adjusting the layer thickness at the nanometer scale results in improved control of the mechanical properties.

(d) Increased versatility of applications subsequent to the development of LBL methods based on intermolecular interactions other than electrostatic.

Furthermore, the LBL assembly does not require only planar substrates as demonstrated by the step-wise build up on a spherical template [84]. However, it does require a surface with the lowest possible roughness since roughness leads to an assembly with poor uniformity and far less stability to electrochemical cycling [85] which inevitably has an adverse affect on the applications.

This relatively new technique already has applications [86] in a few areas which include drug and gene delivery, fuel cells, electrical conductors, photo-detection, biosensing and electrochemical sensing devices. However, this dissertation concentrates on the fabrication of electrochemical sensors via electrostatic interaction using either the self assembly or layer-by-layer assembly processes to incorporate carbon nanotubes, monolayer-protected clusters of gold nanoparticles and MPc complexes.

Given the plethora of potential technological applications of CNTs and MPc complexes and their hybrids, an emerging area of research is on the smart integration of CNTs with MPc complexes for enhancing electrocatalysis and sensing. Reports on the CNT-MPc nanohybrids or thin films have shown these nanohybrids to be more efficient in improving electrochemical responses compared to the bare electrode or the individual CNT or MPc species [87-91]. To improve the physico-chemical properties of MPc complexes for potential nanotechnological applications, continued investigation on their nanostructures are essential. Although there are reports on the self-assembled monolayers (SAMs) of electroactive MPc complexes [92-95] and their CNT hybrids [20], there are limited studies on the use of LBL for electroactive MPc complexes. Indeed, the few reports on LBL involving MPc complexes have been those of Oliveira and co-workers [96-99] who only reported the LBL multilayer films of polyelectrolyte cations with the popular and commercially-available, water-soluble tetrasulphonated MPc complexes using ITO based electrode.

Transition metal tetrasulfophthalocyanine complexes, notably iron (II) tetrasulfophthalocyanine (FeTSPc), are highly water-soluble species and well recognized for their high catalytic activity in homogeneous electrocatalysis. The ease with which they are washed away from electrodes during electrochemical studies has long been a major setback and has limited their fundamental studies and potential applications for heterogeneous electrocatalysis in aqueous environment. To date, all available reports on the surface-confinement of water-soluble metallotetrasulfophthalocyanine (MTSPc, where M = central metal ion) complexes involved indium tin oxide (ITO)-coated glass electrodes and LBL strategy using polycationic and/or highly-branched polymeric complexes such as polyamidoamine (PAMAM) dendrimers [97], poly(diaallyldimethylammonium chloride) (PDDA) incorporating poly(2-(methacryloxy)ethyl)trimethylammonium chloride (PCM), poly(3,4-ethylenedioxythiophene) (PEDOT) and poly(4-styrenesulfonate) (PSS) [100], chitosan [98] and PAMAM [99]. Bedioui and co-workers [87] reported the use of drop-casting to immobilize slurry of nickel (II) tetrasulfophthalocyanine (NiTSPc) and SWCNTs onto a glassy carbon electrode (GCE). The most common feature of the LBL strategies includes the use of a cocktail of relatively expensive reagents and the confinement of the MTSPc inside the thick multi-layered polymeric films. The main problems usually associated with physical anchorage (i.e., drop-casting method) of such films onto a GCE surface are poor stability as well as the difficulty in controlling the amount of film or thickness deposited. These problems have the tendency to compromise on the application of the films. Therefore, it is without doubt very crucial to continue the search for other means of immobilizing them onto electrode surfaces as thin stable solid films without compromising on their electrocatalytic activity towards the detection of analytes in aqueous conditions. More importantly, integrating such water-soluble redox-active MPc complexes with CNTs (as electron transfer mediators) could provide an interesting synergistic means of further enhancing the electron transfer dynamics of MPc complexes.

In this study, using positively-charged 2-dimethylaminoethanethiol monolayer as the base co-ordinating species I show for the first time, the integration of: (i) nanostructed iron (II) phthalocyanine with (a) SWCNT-*poly* (m-amino benzene sulfonic acid); (b) monolayer-protected clusters of gold nanoparticles and (ii) sulfonic acid functionalized iron (II) phthalocyanine with SWCNT-*poly* (m-amino benzene sulfonic acid), singly or mixed immobilization onto gold electrode via. electrostatic interaction either by the conventional self-assembly or the related layer-by-layer assembly strategy. The electron transfer dynamics of such electrodes were interrogated as well as their catalytic properties towards the detection of epinephrine and hydrogen peroxide as analytical probes.

The following three sections further summarize the structure, properties and applications of carbon nanotubes, phthalocyanines and monolayer-protected clusters of gold nanoparticles.

1.3.3 Carbon Nanotube Modified Electrodes

Historical Perspective

The frequently used phrase *"since the discovery of carbon nanotube by Iijima in 1991…"* is a common misconception. A recent editorial by Monthioux and Kuznetsov [101], show that the first Transmission electron microscopy (TEM) images of hollow carbon filaments with a nano-sized diameter were published in 1952 by two Russian scientists, Radushkevich and Lukyanovich [102]. The images of the nano-sized carbon filaments were regarded to be of multi-walled tubular nature but, unfortunately due to the cold war, Russian scientific publications were not easily accessible. Therefore, it is argued that may be they should be credited with the discovery of "carbon nanotubes". However, it is worth mentioning, the concept of forming carbon filaments (through thermal decomposition of gaseous hydrocarbon) was envisaged as early as 1889 [103]. In fact, Iijima's "rediscovery" [104] was at the back of a couple of "carbon nanotube" related reports [102,105]. In 1978, Wiles and Abrahamson [105] grew fine fibres as small as 4 nm in diameter (viz. nanotubes) on graphite and carbon anodes. Nevertheless, Iijima's rediscovery created tremendous impact in the scientific world, probably because it was published in a top-ranked journal that was available to all scientists or perhaps the scientific community was finally ready to accept the concept of *"nano"* in the 1990s. He reported needle-like tubes (fullerene related structures which consist of graphite cylinders closed at either end) while investigating material deposited on the cathode during the arc-evaporation synthesis (Fig. 1.11a) of fullerenes. It was later shown that by varying the conditions of the arc discharge method nanotubes could be produced in bulk quantity [106, 107]. In 1993, Iijima and Ichihashi [108] were unquestionably the first to discover single-walled carbon nanotube. Later that year Yacaman *et al*. [109] used a new technique known as chemical vapour decomposition (CVD) to report the catalytic growth of CNT (Fig. 1.11c) and in 1996 Smalley and co-workers [110] reported the synthesis of bundles of aligned SWCNT by use of the laser-ablation technique (Fig. 1.11b).

From the discoveries made, CNTs are commonly categorised as either SWCNTs or MWCNTs. However, today it is possible to have double walled CNTs [112]. SWCNT shown in Figure 1.12 (a) is essentially formed by rolling a single graphite sheet into a seamless tube capped at each end by half-spherical fullerene structures [113]. They have a diameter of approximately 1-2 nm and a tube length that can be thousands of times more.

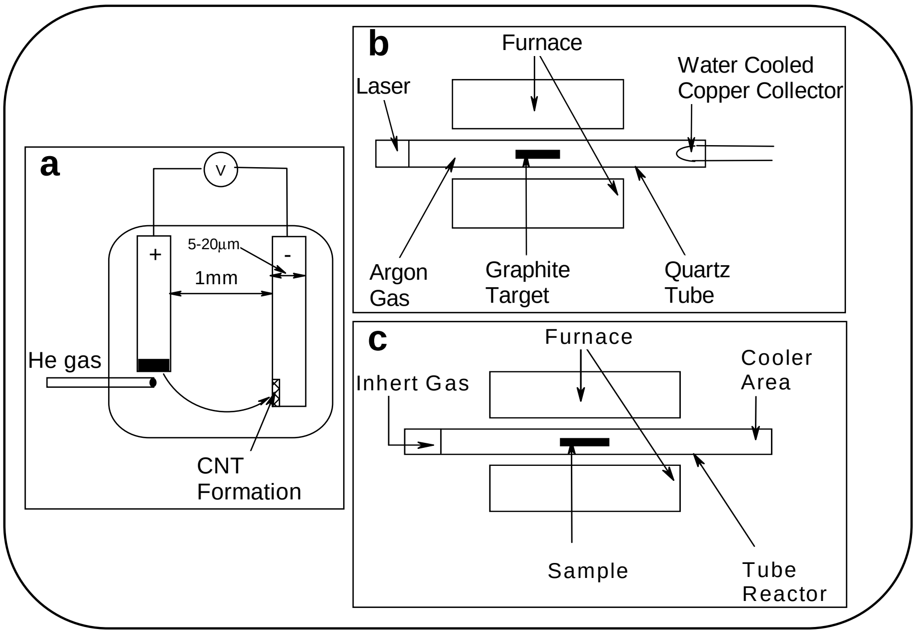

Figure 1.11: Experimental arrangement for synthesizing carbon nanotubes via. (a) Arc-discharge (b) Laser-evaporation (c) Catalytic growth by decomposition of hydrocarbon gas [111].

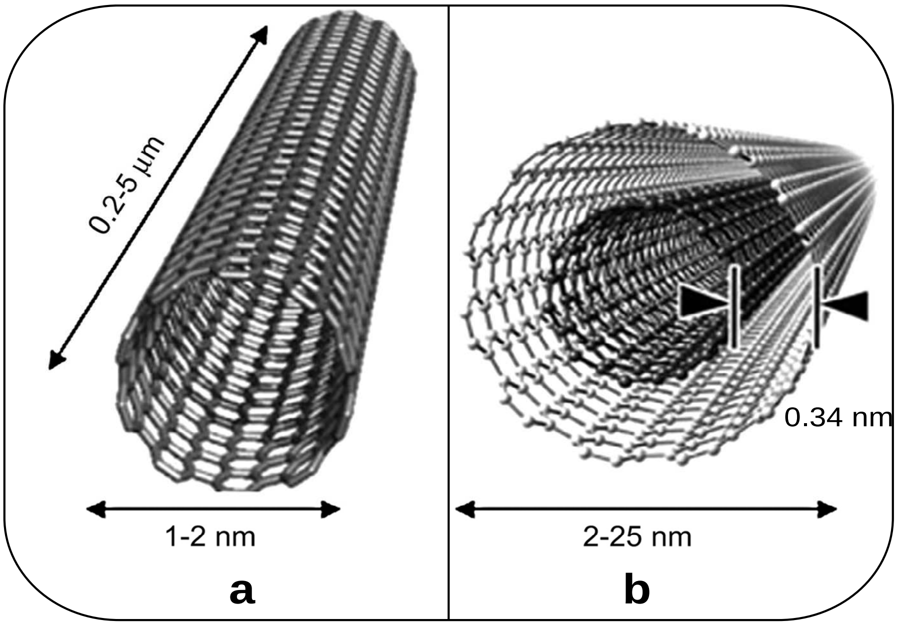

Figure 1.12: Illustration of (a) Single-walled carbon nanotube and (b) Multi-walled carbon nanotube [114(a)].

MWCNT represented in Figure 1.12 (b) comprises of numerous concentric cylinders fitted one inside the other. The number of tubes range from 2-50 graphite cylindrical sheets, with the tubes separated by a distance of 0.34 nm and the innermost tube having a diameter of approximately 1-2 nm [104].

The work described in this dissertation is based on SWCNTs which has received considerable attention for nearly two decades and continued to be investigated as viable electrochemical materials because of their unique properties [111,114-125]. SWCNTs have certain special features over the MWCNTs including smaller size, larger specific area, stronger adsorptive properties and inter-tube attraction [111]. In addition, its characteristic curve-shaped surface enables bonding of supramolecular complexes via non-covalent or hydrophobic interactions [126]. However, in the synthesis process, unlike MWCNTs, SWCNTs requires the use of catalysts [111].

Structure

Carbon nanotubes consist of sp^2 carbon units and the arrangement of the carbon-atom hexagons are in a helical fashion with respect to the needle axis [104]. The three most common structures of carbon nanotubes represented in Figure 1.13 are the (a) armchair, (b) zig-zag and (c) chiral forms. While carbon nanotubes are not actually formed by rolling graphite sheet (graphene) into a tube, the concept can be used to explain the different structures by considering the manner in which graphene might be rolled into tubes. The above mentioned structures can be described by the manner in which the graphene is rolled about the T vector represented in Figure 1.14. Formation of the armchair structure occurs when the graphene is rolled about the T vector parallel to C-C bonds of the carbon hexagons while the zigzag and chiral structures are as a result of the T vector having different orientations except parallel to the C-C bonds [110,111]. This implies that chirality of the tubes is dependent on the direction in which the graphene is rolled in respect to the T vector. The manner in which the graphene is rolled also determines if the CNT is metallic, semi-metallic or semi-conducting [127,128].

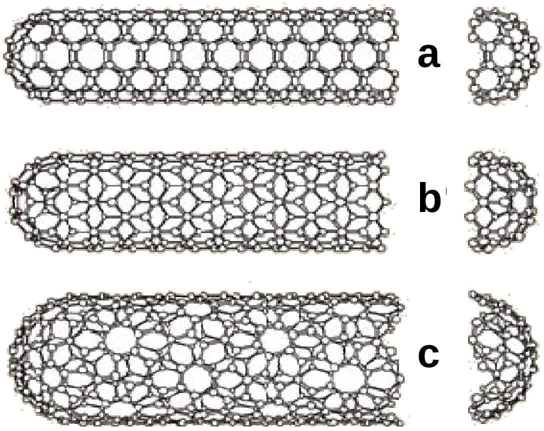

Figure 1.13: Illustration of possible carbon nanotubes structures: (a) Armchair (b), Zigzag and (c) Chiral forms [111].

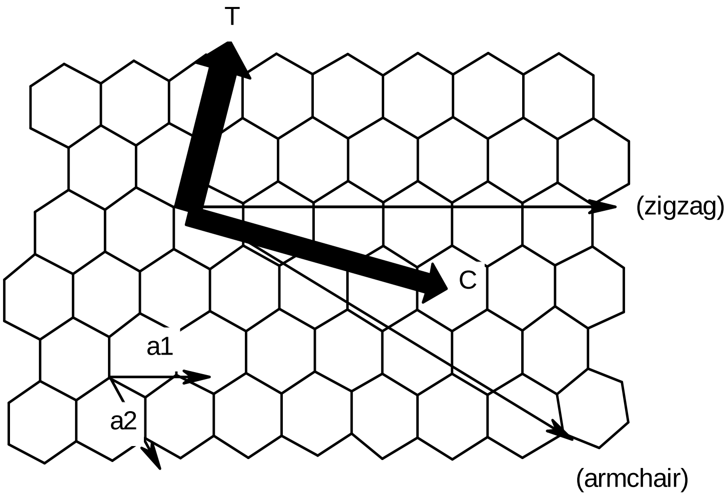

Figure 1.14: Representation of the helical arrangement of an unrolled graphite sheet that can be used to explain carbon tube structures [107]. a_1 and a_2 are the basis vectors of the graphene sheet while C is the circumferential vector.

Pristine CNT can exist as any of these forms. However, functionalization of CNTs is usually required for attachment of CNT to other materials or devices in order to maximise its full potential in various applications. Ever since Smalley's laser-oven functionalization technique [110], there have been numerous reports underlining functionalized CNT modification [129-134]. Functionalization is important to improve solubility [134], especially for potential applications in biology and material science and also to permit the unique properties of carbon nanotubes to be coupled to those of other materials [135]. Carboxylic group [129], fluorine [130], amino [131], alkyl groups [132] and sulfonic groups [133] are a few examples of some of the groups that can be functionalized on carbon nanotubes. In this work, I used SWCNT-*poly* (m-amino benzene sulfonic acid) (SWCNT-PABS).

Properties

Carbon nanotubes has been one of the most extensively studied materials since its “re-discovery” in 1991 owing predominantly to their plethora of properties. One of their most admirable properties due to their limited atomic defects [114(b)] is their ability to demonstrate tremendous mechanical strength [115,116]. In fact, the tensile strength (a measure of the amount of stress required to pull a material apart) of carbon nanotube is approximately 45 billion pascals, which is roughly 20 times more than the tensile strength of steel [111]. Other unique properties of carbon nanotubes include elasticity [116], high thermal conductivity [117(a)], electronic and vibrational properties [117(b)], field emission [118], electrochemical properties [119], optical [120], magnetic [121], photophysical properties [122], morphological and rheological properties [123], pseudocapactive properties [124], ion storage [125] and a high surface area [110] to mention but a few. These properties are often applied to find new applications for carbon nanotubes.

Applications

Since Iijima's rediscovery in 1991, there has been a substantial increase in reports involving CNT investigations (Fig. 1.15) which include over one thousand review articles. A steady increase at an average of ~20% increase per annum means the number CNT publications will exceed 11000 by 2010. The unusual properties of carbon nanotubes have made it possible to frequently find new applications in different fields.

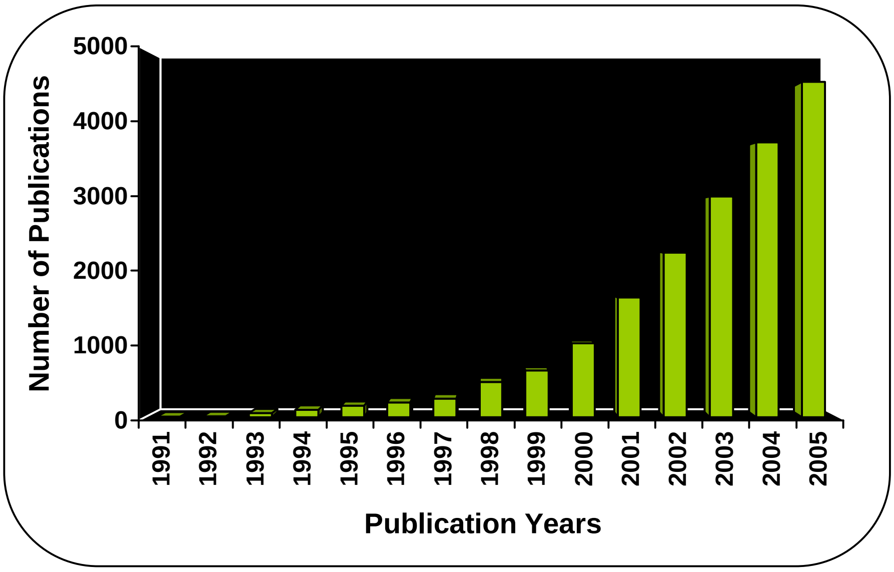

Figure 1.15: 3-D histogram depicting the number of publications concerning carbon nanotubes from 1991-2005 [136].

Some of the applications of carbon nanotubes include their use in the development of artificial muscles [137], as a substitute for the graphite anode in lithium ion batteries [138], as catalyst support in proton-exchange membrane, hydrogen/oxygen and methanol fuel cells

[139-142], battery technology [143], superconductors [144], supercapacitors [145], hydrogen energy storage [146], field-effect transistors [147], catalyst support [148], electronic devices [149], nanotweezers [150] electrochemical energy device [151], ultra high-strength engineering fibers [152], and quantum wires [153], drug and gene delivery systems [154-157], acoustic actuators (speakers) [158], tips for scanning probe microscopy [159], logic circuits in computers [160], chemical sensors [161-163] etc. However, the emphasis here is on the fabrication of electrochemical sensors using carbon nanotubes.

Electrochemical sensors represent a subclass of chemical sensors in which the electrode used meets the size, cost and power requirements. The ability of CNT based electrodes to function as electrocatalysts permit them to operate as electrochemical sensors [164]. In 1996, Britto and co-workers [119] were the first to show that the important neurotransmitter, dopamine could be electrocatalytically oxidised using multi-walled carbon nanotubes modified onto glassy carbon electrodes. A few years later, they used MWCNT microelectrodes in the study of electrocatalytic reduction of dissolved oxygen [165]. In 1997, Davis *et al*. [166] immobilized cytochrome C and azurin proteins on nanotubes to demonstrate the ability of carbon nanotube modified electrodes to act as biosensing devices. In 2001, Li and co-workers [167] catalysed the electrochemical reaction of dopamine, epinephrine and ascorbic acid using carboxyl terminated single-walled carbon nanotubes cast on glassy carbon electrode. The electrocatalytic ability of carbon nanotubes membranes [168], carbon nanotube paste electrodes [169] and carbon nanotubes modified platinum [170] and gold electrodes [171,172] have also been investigated. Other analytes that have been investigated using carbon nanotube based sensors include 3,4-dihydroxy phenylacetic acid [173], nitric oxide [174], NADH [175], serotonin [176], carbohydrates [177], tinidazole [178], DNA [179], homocysteine [180], insulin [181], TNT [182], nucleic acids [183], glucose [184], pesticides [185] and hydrogen peroxide [186]. The performances of these electrodes were found to be superior to other carbon electrodes in terms of promoting electron-transfer and improving reversibility. Nowadays the ability to modify carbon nanotubes with a functional group of interest and use it for the electrochemical detection of any known or unknown analyte is restricted only by the imagination of the electrochemist.

An emerging area of research is on the smart integration of CNTs with metallophthalocyanine (MPc) complexes (to be discussed in the following section) for enhancing electrocatalysis and sensing. Several reports have shown CNT-MPc nanohybrids to be more efficient in improving electrochemical responses compared to the bare electrode or the individual CNT or MPc species [87-95,187-200]. The surprisingly few reports on LBL assembled MPc-CNT films has prompted me to further investigate the electron transport and electrocatalytic behaviour of these self-assembled thin film hybrids.

1.3.4 Metallophthalocyanine Modified Electrodes

Historical Perspective

The first observation of a "phthalocyanine" complex was in 1907 when two German scientists reported the appearance of an unknown blue by-product [201]. Two decades later, researchers from Switzerland tried to convert *o*-dibromobenzene into phthalonitrile but instead synthesized copper phthalocyanine, copper naphthalocyanine and copper octamethylphthalocyanine [202]. In 1928 the "real discovery" of phthalocyanine accidentally occurred during the preparation of phthalimide at the Grangemouth plant of the Scottish Dyes Ltd, which later became part of the Imperial Chemical industries [203]. History has it that during the preparation of phthalimide, a glass lined vessel cracked thereby exposing the reaction to the outer steel casing resulting in the formation of traces of a dark blue impurity in the phthalimide. At the Imperial College, Linstead [204] analyzed these impurities and found it to be iron "phthalocyanine" (FePc), the structure of which was confirmed by Robertson [205,206] using X-Ray diffraction techniques. Linstead named the compound phthalocyanine (*phthalo* from its precursor, 'phthalic acid', and *cyanine* from the greek work 'blue').

Structure and Synthesis

Metallophthalocyanine (MPc) is a planar, 18 π-electron macrocyclic aromatic compound, consisting of four isoindole subunits linked together by aza nitrogen atoms [206,207]. These beautiful bright blue to green coloured materials are biological mimics of the naturally occurring metalloporphyrins but they have extended conjugation due to the benzene rings, hence, improved chemical and thermal stability. The central cavity of its structure (Fig. 1.16a) can enclose any one of 70 metal cations [203] ranging from groups I and II to the lanthanide and actinides [207,208]. Phthalocyanine molecules can also incorporate ring substituents as shown in Figure 1.16 (b). Many of the phthalocyanine properties, example solubility, can be varied by changing the central metal ions and ring substituents [207]. Metallophthalocyanine synthesis is aimed at introducing a metal ion into the central cavity. The synthesis of metallophthalocyanine requires the use of precursors such as phthalic anhydride, diiminoisoindline, phthalonitrile and o-cyanobenzamide [207,209].

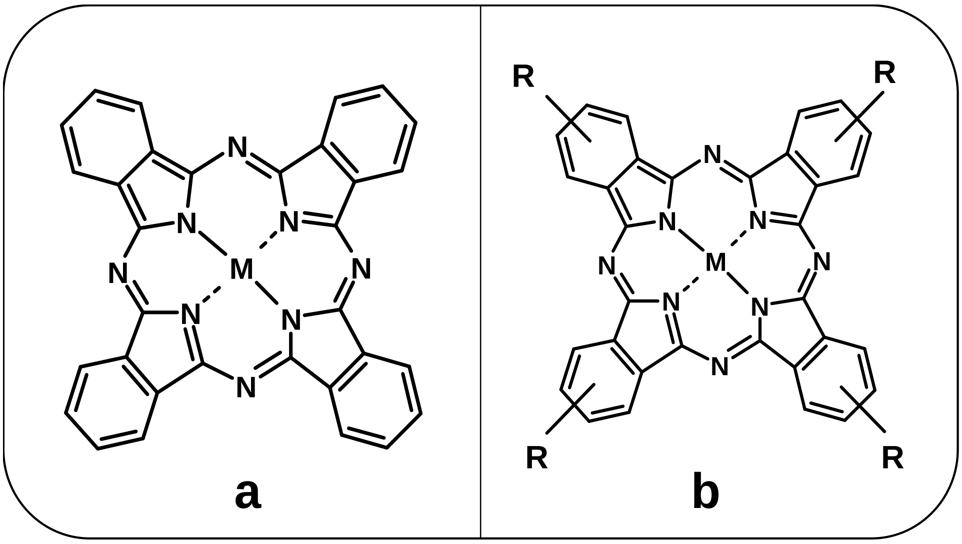

Figure 1.16: The geometric structure of (a) Metallophthalocyanine (b) Metallo-tetraaminophthalocyanine (MTAPc) complex, where M = transition metals (Example: Co, Ni or Fe) and R = (Example: SO_3^{2-}, NH_2, COOH).

Through the years, metallophthalocyanines have established themselves as versatile organometallic complexes with a wide range of excellent properties [210] such as fastness to light, structural, remarkable chemical stability, electronic, optical and beautiful bright blue to green colours etc. However, these properties are size-dependent and can be varied by adjusting the particle size. It is well documented that nanoscopic materials have fundamentally different properties compared to their bulk counterparts [211,212]. The preparation of nanophthalocyanine was first reported in 1991 by two independent groups viz. Saito *et al*. and Enokida *et al*. [213,214]. A few years later nanophthalocyanine was further investigated by Wang *et* *al*. [215] using nanoscopic oxovanadium phthalocyanine. They noticed an improvement in photoconductivity and attributed this to the presence of the huge surface area of nanoscopic oxovanadium nanophthalocyanine.

In this study, the electrocatalytic ability of nano iron (II) phthalocyanine (*nano*FePc) and iron (II) tetrasulphonated phthalocyanines (FeTSPc) will be further investigated. It is anticipated that the emergence of new properties for nanoscopic material will enhance the applications of the macroscopic form.

Applications

Phthalocyanines and related complexes have been one of the most researched areas in science over the last century but their renaissance over the last two decades has lead to an exponentially increasing number of publications (Fig. 1.17), especially in the context of emerging nanoscience and nanotechnology. In the last 20 years, number of publications increased at an average of ~20% /5 year period, meaning that if the same growth persists, then by 2010 it could be predicted to be ~10500 publications. As mentioned earlier, phthalocyanines have a wide range of properties and have been used in the past mainly as dyes for jeans and clothing, inks in ballpoint pens and paints for plastic and metal surfaces.

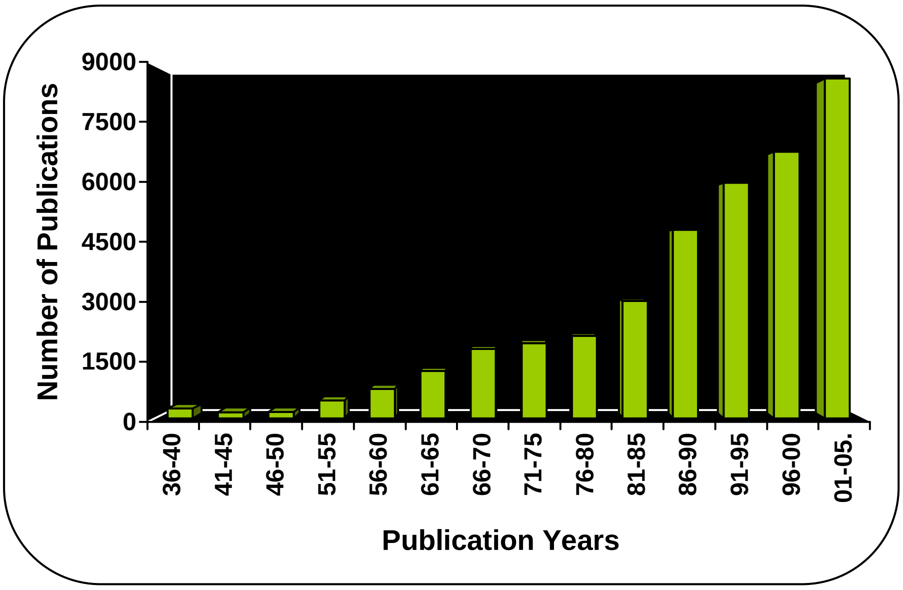

Figure 1.17: 3-D histogram depicting the number of publications concerning phthalocyanines from 1936-2005 [216].

Nowadays they are the molecules of targets for numerous scientific and technological applications in various fields such as catalysis [217-220], sensors [221-223], photodynamic therapy [224-228], ink jet printing [229], electrophotography [229,230], photocopying and laser printing [229,231], electrochromic display devices [232-234], optical computer re-writable discs and information storage systems [235-237], liquid crystal display devices [238], photovoltaic cells [239,240], fuel cells [241], molecular electronics [242], semi-conductor devices [243-245], and electrochemical sensors [187-200]. A recent review by de la Torre *et al*. [216] discusses several reasons for their involvement in some of the above listed applications but the focus remains on the fabrication of electrochemical sensors using nano iron (II) phthalocyanine and iron (II) tetrasulphonated phthalocyanines.

MPc complexes have the ability to retain their molecular structure and stability upon addition or removal of electrons [246] which enables them to exhibit electrocatalytic activity towards redox reactions. Thus they have established themselves as excellent electrocatalysts for several organic and inorganic analytes [247-251] and have recently been reviewed by Ozoemena and Nyokong [252]. In contrast there has been limited work relating to the electrocatalytic ability of nanostructured MPc complexes [253,254] which is surprising given their potential to enhance the electrochemical response. However, I believe that the electrochemical response can be further enhanced by integrating nanostructured MPc complexes with other redox active material such as SWCNTs and monolayer-protected clusters of gold nanoparticles. Indeed, previous studies [89, 90] have shown it has been shown MPC-CNT hybrids exhibit excellent electrocatalysis and sensing. However, there is no work yet on MPC-MPCAuNP.

1.3.5 Monolayer-Protected Clusters of Gold Nanoparticles Electrodes

Historical Perspective

Solid gold was first extracted in the 5th millennium B.C. in Bulgaria; whereas soluble gold is believed to have been in existence from the 5th or 4th century B.C. when it was used to make ruby glass and for colouring ceramics. The procedure for making gold ruby glass also known as "Purple of Cassius" [255] was described by Andreus Cassius in 1685. Its beautiful colour was often suspected to be a gold tin compound that may have been formed as a result of the starting material used in the preparation process [256]. However, in 1857, Faraday reported the formation of a deep red gold solution when he used white phosphorous to reduce an aqueous solution of chloroaurate ($AuCl_4^-$) and attributed the colour of ruby glass to the minute size of the gold particles [257]. This discovery reiterated a statement made by Kunchel in 1676 [258], where he claimed "gold must be present in such a degree of communition that it is not visible to the human eye". A few years after Faraday's discovery, in 1861, the term colloid [259] was derived to describe dispersion of one substance in another and as a result gold in solution. Colloidal gold, gold colloid or soluble gold was also referred to as gold nanoparticles or nano gold after Norio Taniguchi [260] coined the term nanoparticle in 1974. The term was used to describe any kind of particle that has at least one dimension in the range of 1 - 100 nm. More than a century after Faraday's initial discovery, Murray and Chen [261] showed it was possible to attach alkanethiols to "gold nanoparticles". A few years later, gold nanoparticles surrounded by a thiol monolayer were termed monolayer-protected gold cluster molecules [262] also known as monolayer-protected clusters of gold nanoparticles (MPCAuNP).

Structure and Synthesis

Gold colloids are routinely prepared by chemical reduction of a suitable gold precursor such as $AuCl_4^-$ ions and there are several reducing agents that can be used to achieve nanoparticles from this precursor. As mentioned earlier, Michael Faraday first used white phosphorous to reduce an aqueous solution of $AuCl_4^-$. Since then there have been several routes using different reducing agents to prepare nanosized gold colloids. However, only two preparation techniques have become well established. One of the most widely used methods is the innovative two-phase Brust-Schiffrin method [263], where aqueous sodium borohydride is used to reduce $AuCl_4^-$ in toluene in the presence of stabilizing thiols. Thiolate ligands are attached to provide superior stability. The strong interaction between the sulphur of the thiolate ligands and the gold facilitates the formation of a protective shell around the particle which is responsible for this stability.The other reliable method is the older Turkevich synthesis [264], where gold salt is boiled together with citrate to get 10-15 nm water-soluble particles.

MPCAuNP used in this work was supplied by Mintek (South Africa) and synthesised by treating citrate-stabilised gold with a mixture of carboxyl and hydroxyl polyethylene glycol (PEG) ligands. Scheme 1.2 shows a cartoon representation of the reaction. To my knowledge, this dissertation reports the first time (i) their self assembled nano-thin films and (ii) their electrochemical integration to investigate their heterogeneous electron transport behaviour as well as their electrocatalytic ability.

The most widely investigated family of ligands are thiolates (RS^-, R = organic moiety), frequently derived from organic thiols and disulfides. The strong interaction between the sulphur of the thiolate ligands and the gold surface facilitates the formation of a protective shell around the particle which (i) improves the stability by preventing uncontrolled aggregation of the particles and (ii) furnishes the nanoparticle with additional functionality, such as electronic, optical, thermal, catalytic, sensor, biomolecular recognition or transport properties [265,266] for potential applications in the fields of physics, chemistry, biology, medicine, and material science [267].

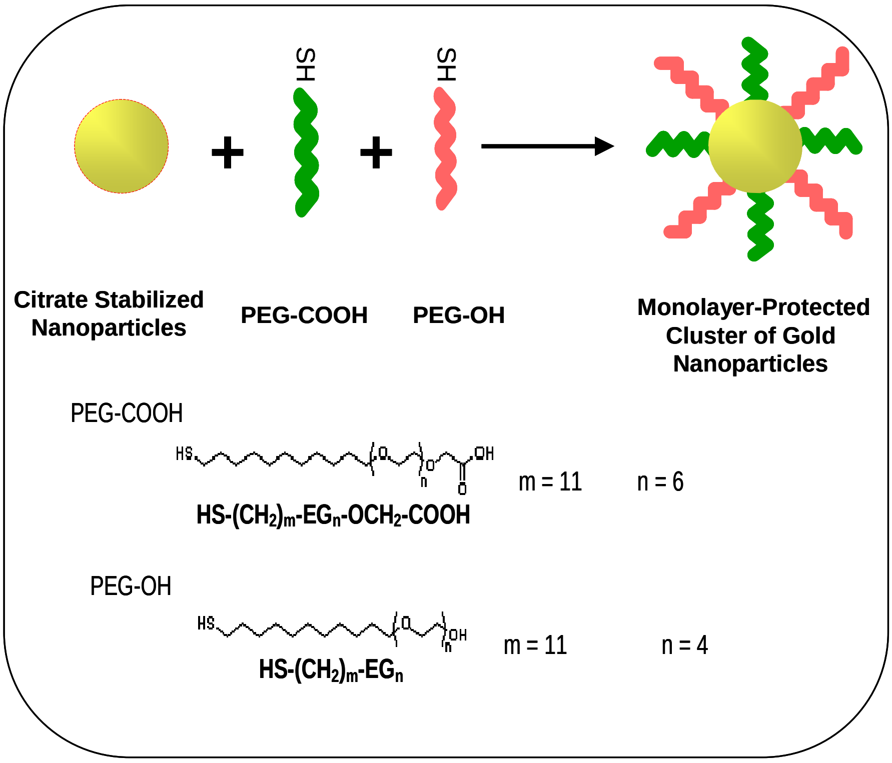

Scheme 1.2: Reaction scheme illustrating the one-step stabilization and functionalization of gold nanoparticles with carboxyl and hydroxyl PEG ligands.

Applications

The significant amount of work carried out in the field on monolayer-protected clusters of gold nanoparticles have already found a wide range of applications in nonlinear optical devices, electrophoresis, optoelectronic devices, fluorescence, catalysis, biochemistry, drug delivery and sensors [268-270]. However, in this study I investigated the electron transport properties and electrocatalytic behaviour of SAM modified electrochemical sensors, where this time

MPC of gold nanoparticles were used as the modifier in this fabrication process. MPCAuNP have been used for nanotechnology applications since the development of the Au_{55} cluster by Schmid *et al*. in 1981 [271]. In 1996, the Brust-Schiffrin group [272] studied 1,9 nonanethiol ($HS(CH_2)_9SH$) derivatized gold nanoparticles towards $[Fe(CN)_6]^{4-/3-}$. The layer-by-layer assembly of gold clusters and nonanethiol promoted and impeded the electrode's ability, respectively. Consequently, there was an increase in the rate of electron transfer when gold clusters were used as the outer layers and a decrease following nonanethiol assembly. However, it was work done by Murray's group in 1998 that led to an influx of investigations describing the electron transport behaviour of MPCAuNPs. They used gold clusters modified with anthraquinone to demonstrate the enhancement of 1,1 –dinitrocyclo-haxane reduction [273,274] and described MPCAuNP as multivalent redox species that can store charge. A year later, Zhong *et al*. [275] showed that rate of electron transfer between gold nanoparticles immobilized on dithiol gold substrates depend on (i) the arrangement of the nanoparticles and (ii) the distance between the underlying electrode and the gold nanoparticles. Musick *et al*. [276] investigated the impact of numerous layers of gold clusters modified onto dithiol electrodes. When less than seven layers were used, the wave shaped voltammogram indicated that the electrode functioned as independent microelectrodes in a blocking film, while the peak shaped voltammograms observed for more than seven layers indicated a planar diffusion controlled process of the solution probe to the electrode. Hu *et al*. [277] also reported the presence of peak shaped voltammograms when he investigated the behaviour of gold clusters immobilized on cysteamine assembled gold surface towards the $[Fe(CN)_6]^{4-/3-}$ redox probe. In 2000, Chen [278] reported the electron transfer behaviour using CV and impedance measurements of a dithiolate MPCAuNP monolayer assembled directly onto the gold surface. Hicks *et al*. [279] also used electrochemical impedance spectroscopy to investigate the electron transport properties of a mixed monolayer (hexanethiolate/ mercaptoundecanoic (MUA)) MPCAuNP attached to MUA-functionalized gold electrode. Bharathi *et al.* [280] incorporated gold nanoparticles in to a silicate network to promote the rate of electron transfer. Maye *et al*. [281] assembled decanthiolate protected gold clusters on 1,9-nonanedithiol and 11-mercaptoundecanoic acid substrates to demonstrate the amplification of methanol oxidation. In contrast, Yang and Zhang [282] found no improvement in the electronic communication between the solution species: $Fe(CN)_6^{3-}$ or $Ru(NH_3)_6^{3+}$ and the underlying gold electrode surface subsequent to the attachment of gold nanoparticles to 1,6-hexanedithiol and 1,9- nonanedithiol modified electrodes. In

2004, Toyota *et al*. [283] studied the charging-discharging aspects of gold nanoparticles immobilized on amine-terminated siloxane on an Indium tin oxide electrode. In 2007, Jensen *et al*. [284] showed that gold nanoparticles can act as efficient redox relay for cytochrome c assembled at gold electrodes. Recently enhanced electron transport properties of MPCAuNP modified electrodes were investigated using scanning electron microscopy [285] and temperature [286] techniques. Therefore, nowadays it is well known that electrodes decorated with MPCAuNP mostly improve the electron transport behaviour.

Typical sizes of MPCAuNPs range from 1 to 40 nm depending on the preparation technique. Considering most preparation techniques produce MPCAuNPs that are insoluble in water, it should perhaps not be surprising that there are limited reports on the electron transfer properties and electrochemical biomolecular recognition properties of MPCAuNPs in aqueous media [287]. Thus, for electro-bioanalytical applications, it is essential to develop MPCAuNP systems that are stable, water soluble and capable of molecular recognition in aqueous media.

This work reports for the first time the surface electrochemistry of these stable, yet chemically versatile water-soluble MPCAuNPs self-assembled on polycrystalline electrode disk in terms of their (i) heterogeneous electron transfer dynamics in aqueous and non-aqueous media, (ii) surface ionization properties, and (iii) voltammetric recognition properties towards epinephrine and ascorbic acid. These new MPCAuNPs were prepared by varying the ratio of its two different stabilizing ligands, (1-sulfanylundec-11-yl) polyethylene glycolic acid (herein abbreviated as PEG-COOH) and (1-sulfanylundec-11-yl) tetraethylene glycol (abbreviated as PEG-OH). The extent to which these ratios of protecting ligands influence heterogeneous electron transport and surface pK_a is crucial for the potential applications of such platforms in many areas such as molecular electronics as well as chemical and biological sensing. Here, it is clearly shown that mixtures of different stabilizing ligands have distinct impacts on their electron transfer dynamics in aqueous and non-aqueous media as well as their electrochemical recognition properties towards biologically relevant analytes, epinephrine and ascorbic acid. The importance of catecholamine neurotransmitters (e.g., epinephrine) in the body has been well documented [288-289]. However, the most common challenge in the electroanalytical detection of epinephrine in body fluids is the interference by ascorbic acid; the oxidation peaks of epinephrine and ascorbic acid are very close at physiological pH environment which often results in their voltammetric peaks overlapping thereby inhibiting the detection of epinephrine.

1.4 Species Investigated as Probe Analytes

1.4.1 Epinephrine

In 1886, William Bates reported the discovery of a substance produced by the adrenal gland in the New York Medical Journal. The substance better known as epinephrine (Fig. 1.18) was first isolated in 1895 by Napoleon Cybulski.

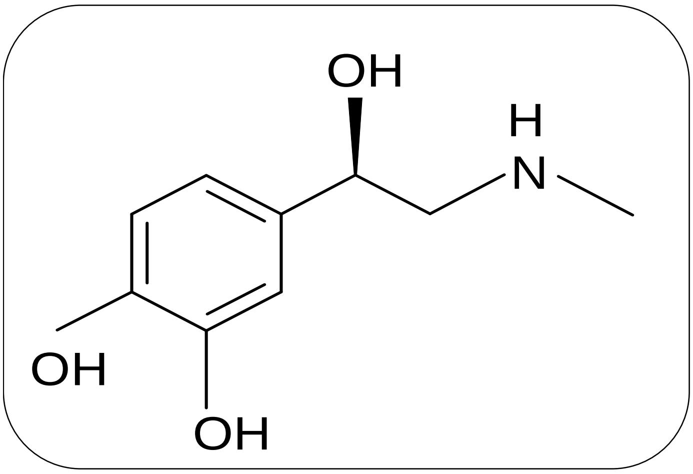

Figure 1.18: Structure of Epinephrine.

It is a catecholamine neurotransmitter commonly referred to as adrenalin or "fight or flight" hormone, derived from the amino acids phenylalanine and tyrosine and released from the adrenal gland in emergency situations. It is an important component of the mammalian central nervous system that exists as large organic cations in the body fluid and the nervous tissue, where it controls the nervous system in the performance of a series of biological reactions and nervous chemical processes [290]. This means the concentration of EP affects processes such as heart rate, blood pressure, contraction of smooth muscles, glycogenolysis in liver and muscle, lipolysis in adipose tissue etc. [291]. Therefore, the detection and analysis of EP is of significant importance for improved pharmacological research and a better understanding of the effects of the nervous system. The determination of epinephrine has been reported with the use of chromatographic methods [292,293], capillary electrophoresis [294,295], spectroscopic methods [296,297], chemiluminescence [298,299], flow injection analysis [300,301] and various electrochemical methods [302-309].

However, the major challenge in epinephrine analysis is the elimination of interferences from ascorbic acid; the oxidation peaks of epinephrine and ascorbic acid are very close which often results in their peaks overlapping. The pK_a values of the hydroxyl groups of epinephrine are 8.7, 9.9 and 12.0, respectively [310,311], while the pK_a of the amino H of epinephrine is reported to be 9.9 [312]. This implies that at the physiological pH epinephrine remains neutral whereas ascorbic acid with pK_a values of 4.17 and 11.5 exists primarily as a monohydrogen ascorbate anion. Wang *et al.* [313] used negatively charged nafion isomer to repel the ascorbic acid but their electrode showed low sensitivity.

However, EP detection with high selectivity and sensitivity remains a major challenge in electroanalytical research [314,315] since EP exists together with ascorbic acid in the biological environment, and AA is oxidized at a similar potential to EP thus resulting in an overlapping voltammetric response. This problem may be resolved by either separating the electrochemical response of EP and AA [315] or eliminating the AA interference altogether [314].

1.4.2 Hydrogen Peroxide

The choice of this analyte stems from the knowledge that FePc is a natural mimic of the iron-containing proteins such as the horseradish peroxidase (HRP) and cytochrome C (cyt C) known for their redox-mediating role in the detection of H_2O_2. Given the high cost, temperature and stability constraints of these biomolecules for use in the detection of hydrogen peroxide (H_2O_2), it is reasonable that a much cheaper, highly stable (chemically and thermally) and easily available nanostructured FePc species could be an admirable alternative redox-mediator.

It is a pale blue liquid which appears colourless in dilute solutions and its strong oxidising properties make it a powerful bleaching agent. It was first isolated in 1818 by Louis Jacques Thénard upon reacting barium peroxide with nitric acid [316]. This process was used until the middle of the 20th century. Nowadays, this molecule is known to be the by product of several biological and enzyme-catalysed reactions (oxidases) and since it is difficult to obtain an accurate measure of biological material present in the body, H_2O_2 is often measured as an indirect indication of the starting material. A common example is the detection of glucose:

$$\text{Glucose} + O_2 \xrightarrow{\text{Glucose oxidase}} \text{Gluconic acid} + H_2O_2 \qquad 1.16$$

In the oxidation of glucose to gluconic acid in the presence of glucose oxidase, the amount of glucose is indirectly detected using the direct detection of the by-product, H_2O_2. Therefore, the need for a high selectivity and extremely sensitive H_2O_2 sensor in food industry, environmental waste and medical diagnosis is of significant importance.

1.5 Microscopic and Spectroscopic Techniques

1.5.1 Scanning Electron Microscopy

Scanning electron microscopy (SEM) is a surface technique employed by the scanning electron microscope to image the surface of samples by scanning it with a high-energy beam of electrons in a raster scan manner. There is an interaction between these electrons and the atoms of the sample, resulting in signals that contain information about the sample's surface topography and composition [317]. In 1935, Max Knoll obtained the first SEM image of silicon steel showing electron channeling contrast [318]. In 1937, Manfred von Ardenne further investigated the beam specimen interactions and the physical principles of the SEM [319,320]. The operation of the SEM is as follows: At the top of a SEM column an electron gun generates a beam of electrons which are attracted through the anode, condensed (condenser lens) and focused (objective lens) as a fine point onto the sample. These electrons are collected by a secondary detector or a backscatter detector. The secondary electron detector produces a clear and focused topographical image of the sample whereas the backscatter electron detector reflects an elemental composition of the sample and is used for energy dispersive X-ray analysis [317,321].

1.5.2 Energy Dispersive X-Ray

Energy dispersive X-ray also referred to as an electron spectroscopy for chemical analysis, is an electron spectroscopic method used to determine the elemental and chemical composition of materials on metal surfaces [322]. The presence of the desired elements in the film can be confirmed using the EDX spectra and evaluating the atomic composition [323]. EDX is based on the photoelectron effect [322] where the surface is irradiated with photons. When incoming primary electrons bombard target material electrons an X-ray photon, characteristic of its own atom (element) is released [324]. Thus measuring the energy lost as a result of secondary electrons being displaced from the primary beam, the corresponding element to that energy loss may be determined.

An atom has a conventional sequence of electrons known as 'electron shells' arranged around its nuclei as a result of electrical charge differences between them. The shells are, also conventionally, labeled K, L, M, N, O, P, and Q from innermost to outermost. Primary electrons strike the atom (Fig. 1.19 a), and knock electrons out of their shell. As a result the atom is excited to higher energy state and relaxes after the ‘knocked out’ electrons are replaced with outer shell electrons. Therefore, there is a difference in energy states where the excess energy can be released in the form of an X-ray, which carries this energy difference, and has a wavelength that is characteristic of the atomic species from which it came. This same process can occur with the L and M electrons and as a result leads to a large number of generated X-rays of differing wavelengths and hence a number of possible lines of X-rays available for analysis [322-323]. A spectrum (Fig. 1.13 b) is an accumulation of an index of X-rays collected from a particular spot on the sample surface each X-ray generated from an element are characteristic of that particular element and can thus be used to identify elements that are truly present under the electron probe [322].

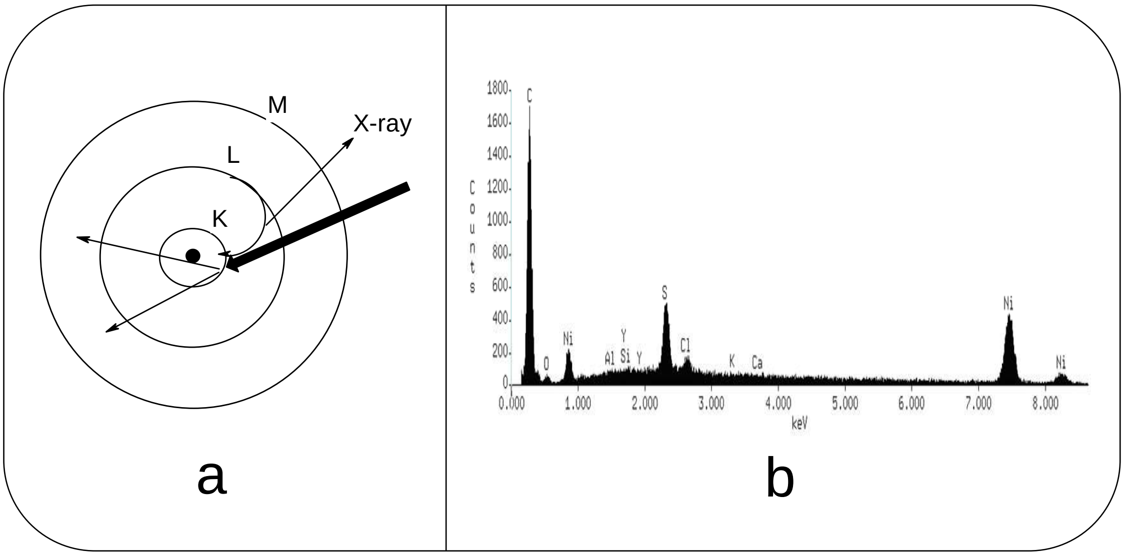

Figure 1.19: Simple representation of the first three shells showing, (a) the formation of energy dispersive X-ray resulting in (b) a unique spectrum.

1.5.3 Atomic Force Microscopy

Atomic force microscopy is a surface characterization technique that uses a sharp probe to scan across a sample detecting interactions between the silicon tip and the conductive or insulating sample resulting in nanoscale resolutions. The acronym AFM also refers to atomic force microscope which is the instrument used for the above mentioned technique. The first AFM was developed by Binnig, Quate and Gerber in 1986 [325]. Atomic force microscopy can be sub-divided into contact mode, acoustic AC mode and magnetic AC mode. Acoustic AC mode was exclusively used during this project because the samples used are not magnetic and unlike contact mode it does not drag across the sample. It essentially monitors the amplitude of a vibrating cantilever, by bouncing a laser beam off it and onto a detector, as it raster scans across the sample using a piezoelectric scanner. The fixed end of the cantilever is moved up and down in the Z direction by the piezoelectric scanner as it raster scans across the surface in the X and Y direction with the aid of a feedback mechanism employed to adjust the “tip-to-sample distance” in order to maintain constant amplitude and hence constant force derivative. The Z position of the tip at each data point in the X-Y plane produces the topographic image of the surface. Most of the surface characterizations in this project make use of the AFM because unlike the SEM which provides a two-dimensional image of the sample, it provides a true three-dimensional surface profile. In addition the AFM functions perfectly in air or liquid environments and the samples viewed by AFM do not require special treatments like carbon coating whereas the SEM requires an expensive vacuum chamber for proper operation.

1.5.4 Transmission Electron Microscopy

Transmission Electron Microscopy (TEM) is a technique operated at a high resolution where the electron is transmitted through the sample owing to the interest in internal detail thus revealing the morphology (size, shape and arrangement of the particles), the crystallographic information (the atom arrangement) and the compositional information (the elemental composition) of the material examined [326-327]. The operation of a TEM is similar to that of a slide projector; however, it shines a beam of electrons, instead of light, generated from an electron gun. This stream of electrons is focused by a coherent beam that is restricted by a condenser aperture. The beam striking the sample transmits portions of the sample which are focused by the objective lens into an image that is projected onto a screen. There are dark and light areas of the image representing the more densely packed section which allowed fewer electrons to pass through and the less densely packed section which allowed more electrons to pass through, respectively [326-327].

Reference:

1. A. E. Kaifer, M. Gómez-Kaifer, *Supramolecular Electrochemistry*, Wiley-VCH, New York, 1999.
2. J. Wang, *Analytical Electrochemistry*, VCH Publishers Inc., New York, 1994.
3. A.J. Bard, L.R. Faulkner, *Electrochemical Methods: Fundamentals and Applications, 2nd ed.*, John Wiley & Sons, Hoboken, NJ, 2001.
4. J.J.T. Maloy in: P.T. Kissinger and W.R. Heineman (Eds.), *Laboratory Techniques in Electroanalytical Chemistry*, Marcel Dekker Inc., New York, 1996.
5. R.G. Compton, C.E. Banks, *Understanding Voltammetry*, World Scientific Publishing Co., Singapore, 2007.
6. V.J. Puglisi, A.J. Bard, J. *Electrocem. Soc*. 119 (1972) 833.
7. F.M. Hawkridge in: P.T. Kissinger and W.R. Heineman (Eds.), *Laboratory Techniques in Electroanalytical Chemistry 2nd ed.*, Marcel Dekker Inc., New York, 1996.
8. D.B. Hibbert, *Introduction to Electrochemistry*, Macmillan, London, 1993.
9. J. E. B. Randles, *Trans. Faraday Soc*. 44 (1948) 327.

10. P.A. Christenson, A. Hamnet, *Techniques and Mechanisms in Electrochemistry*, *1st ed.*, Blackie Academic and Professional, London, 1994.

11. R. S. Niccholson, *Anal. Chem*. 37 (1965) 1351.

12. E. R. Brown, R. F. Large in: A. Weissberger and B. Rossiter (Eds.), *Physical Methods of Chemistry. Electrochemical Methods Vol.1-Part IIA*, Wiley-Interscience, New York, 1971.

13. G. C. Barker, I. L. Jenkins, *Analyst* 77 (1952) 685.

14. J.G. Osteryoung, *Acc. Chem. Res*. 26 (1993) 77.

15. J. Wang, D.B.Luo, P.A.M. Farias, J.S. Mahmoud, *Anal. Chem.* 57 (1985) 158.

16. M.H. Pournaghi-Azar, R. Sabzi, *J. Electroanal. Chem*. 543 (2003) 115.

17. P. Santhosh, K.M. Manesh, K.-P. Lee, A.I. Gopalan, *Electroanalysis* 18 (2006) 894.

18. K.M. Manesh, P. Santhosh, A.I. Gopalan, K.-P. Lee, *Electroanalysis* 18 (2006) 1564.

19. B. Agboola, T. Nyokong, *Talanta* 72 (2007) 691.

20. K. I. Ozoemena, T. Nyokong, D. Nkosi, I. Chambrier, M. J. Cook, *Electrochim. Acta* 52 (2007) 4132.

21. J.R. Macdonald, W.B. Johnson in: E. Barsoukov, J.R. Macdonald (Eds.), *Impedance Spectroscopy, 2nd ed.*, John Wiley and Sons Inc., NJ, 2005.

22. K.A. Joshi, M. Prouza, M. Kum, J. Wang, J. Tang, R. Haddon, W. Chen, A. Mulchandani, *Anal. Chem.* 78 (2006) 331.

23. O.V. Shulga, C. Palmer, *Anal. Bioanal. Chem*. 385 (2006) 1116.

24. S. Krause in: A.J. Bard, M. Stratmann, P.R. Ulwin (Eds.), *Instrumentation and Electroanalytical Chemistry Vol.3*, Wiley-GmbH & Co., 2003.

25. M.A.C. Brett, A.M. O. Brett, *Electrochemical Principles, Methods and Applications*, Oxford University Press, New York, 1993.

26. IUPAC Recommendation, *Pure and Appl. Chem*. 69 (1997) 1317.

27. R. F. Lane, A. T. Hubbard, *J. Phys. Chem*. 77 (1973) 1401.

28. C. M. Elliot, R. W. Murray, *Anal. Chem*. 48 (1976) 1247.

29. C.R. Martin, C.A. Foss Jr. in: P.T. Kissinger and W.R. Heineman (Eds.), *Laboratory Techniques in Electroanalytical Chemistry 2nd ed.*, Marcel Dekker Inc., New York, 1996.

30. L. Netzer, J. Sagiv, *J. Am. Chem. Soc.* 105 (1983) 674.

31. B.F. Watkins, J.R. Behling, E. Kariv, L.L. Miller, *J. Am. Chem. Soc*. 97 (1975) 3549.

32. N. Diab, J. Oni, W. Schuhmann, *Bioelectrochemistry* 66 (2005) 105.

33. C. Deng, M. Li, Q. Xie, M. Liu, Y. Tan, X. Xu, S. Yao, *Anal. Chim. Acta* 557 (2006) 85.

34. Z. Chen, Y. Zhou, *Surface & Coatings Technology* 201 (2006) 2419.

35. S. Pyun, J-S. Bae, *J. Power Sources* 68 (1997) 669.

36. C. Sivakumar, J-N. Nian, H. Teng, *J.Power Sources* 144 (2005) 295.

37. E. Mun˜oz, M. A. Heras, A. I. Colina, V. Ruiz, J. Lo´pez-Palacios, *Electrochim. Acta* 52 (2007) 4778.

38. K. B. Blodgett, *J.Amer. Chem. Soc.* 56 (1934) 495.

39. A. J. Bard, *J. Chem. Ed*. 60 (1983) 303.

40. J.J. Gooding, D.B. Hibbert, *TrAC* 18 (1999) 52.

41. H. O. Finklea in Encyclopedia Chemistry, A. J. Bard and I. Rubinstein, Eds., Marcel Dekker: New York, 1996, Vol.19, pp109-335.

42. I. Langmuir, *J. Am. Chem. Soc.* 39 (1917) 1848.

43. W.C. Bigelow, D.L. Pickett, W.A. Zisman, *J. Colloid interface Sci.* 1 (1946) 513.

44. J. Sagiv, *J. Am. Chem. Soc.* 102 (1980) 92.

45. D.L. Allara, R.G. Nuzzo, *Langmuir* 1 (1985) 45.

46. R.G. Nuzzo, D.L. Allara, *J. Am. Chem. Soc.* 105 (1983) 4481.

47. R.G. Nuzzo, F.A. Fusco, D.L. Allara, *J. Am. Chem. Soc.* 109 (1987) 2358.

48. H.O. Finklea, S. Avery, M. Lynch, T. Furtsch, *Langmuir* 219 (1987) 365.

49. E. Sabatani, I. Rubinstein, *J. Phys. Chem.* 91 (1987) 6663.

50. L. Strong, G.M. Whitesides, *Langmuir* 4 (1988) 546.

51. F. Caruso, E. Rodda, D.N. Furlong, V. Haring, *Sens. Actuators B* 41 (1997) 189.

52. C-J. Zhong, R.C. Brush, J, Anderegg, M.D. Porter, *Langmuir* 15 (1999) 518.

53. K. Nishiyama, S-I., Tahara, Y. Uchida, S. Tanoue, I. Tangiguchi, *J. Electroanal. Chem.* 478 (1999) 83.

54. C.D. Bain, E.B. Troughton, Y-T. Tao, J. Eval, G.M. Whitesides, R.G. Nuzzo, *J. Am. Chem. Soc.* 111 (1989) 321.

55. R.L. Garell, J.E. Chadwick, D.L. Severance, N.A. McDonald, D.C. Myles, *J. Am. Chem. Soc.* 117 (1995) 11563.

56. X. Zhang, H. Chen, H. Zhang, *Chem. Commun.* (2007) 1395.

57. R.K. Iler, *J. Colloid Interface Sci.* 21 (1966) 569.

58. G. Decher, J.D. Hong, *Makromol. Chem. Macromol. Symp.* 46 (1991) 321.

59. G. Decher, J.D. Hong, *Ber. Bunsen-Ges. Phys. Chem.* 95 (1991) 1430.

60. Y. Lvov, G. Decher, H. Mohwald, *Langmuir* 9 (1993) 481.

61. G. Decher, Y. Lvov, J. Schmitt, *Thin Solid Films* 244 (1994) 772.

62. J. C. Jan, M.D. Walton, E.P. McConnell, W.S. Jang, Y.S. Kim, J.C. Grunlan, *Carbon* 44 (2006) 1974.

63. S.S. Shiratori, M.F. Rubner, *Macromolecules* 33 (2000) 4213.

64. H.N Zhang, J. Ruhe, *Macromolecules* 36 (2003) 6593.

65. R. A. McAloney, M. Sinyor, V. Dudnik, M.C. Goh, *Langmuir* 17 (2001) 6655.

66. O. Mermut, C.J. Barrett, *J. Phys. Chem. B* 107 (2003) 2525.

67. Z. J. Sui, D. Salloum, J.B. Schlenoff, *Langmuir* 19 (2003) 2491.

68. H.L. Tan, M.J. McMurdo, G.Q. Pan, P.G. Van Patten, *Langmuir* 19 (2003) 9311.

69. A.C. Fou, O. Onitsuka, M. Ferreira, M.F. Rubner, B.R. Hsieh, *J. Appl. Phys.* 79 (1996) 7501.

70. W.B. Stockton, M.F. Rubner, *Macromolecules* 30 (1997) 2715.

71. M. Raposo, R.S. Pontes, L.H.C. Mattoso, O.N. Oliveira Jr., *Macromolecules* 30 (1997) 6095.

72. S.W. Keller, H.N. Kim, T.E. Mallouk, *J. Am. Chem. Soc.* 116 (1994) 8817.

73. D.E. Cliffel, F.P. Zamborini, R.W. Murray, *Langmuir* 16 (2000) 9699.

74. F. Caruso, W.J. Yang, D. Trau, R. Renneberg, *Langmuir* 16 (2000) 8932.

75. E. Donath, G.B. Sukhorukov, F. Caruso, S.A. Davis, H. Mohwald, *Angew. Chem. Int. Ed.* 37 (1998) 2202.

76. B.G. De Geest, R.E. Vandenbroucke, A.M. Guenther, *Adv. Mater.* 18 (2006) 1005.

77. F. Caruso, D. Trau, H. Mohwald, R. Renneberg, *Langmuir* 16 (2000) 1485.

78. W. Shan, H. Liu, J. Shi, L. Yang, N. Hu, *Biophysical Chem.* 134 (2008) 101.

79. Y. Lvov, G. Decher, G. Sukhorukov, *Macromolecules* 26 (1993) 5396.

80. V. Zucolotto, K.R.P. Daghastanli, C.O. Hayasaka, A. Riul, P. Ciancaglini, O.N. Oliveira Jr., *Anal. Chem.* 79 (2007) 2163.

81. M. Olek, J. Ostrander, S. Jurga, H. Mohwald, N. Kotov, K. Kempa, M. Giersig, *Nano Lett.* 4 (2004) 1889.

82. V. Zucolotto, M. Ferreira, M.R. Cordeiro, C.J.L. Constantino, D.T. Balogh, A.R. Zanatta, W.C. Moreira, O.N. Oliveira Jr. *J. Phys.Chem. B* 107 (2003) 3733.

83. A.C. Templeton, W.P. Wuelfing, R.W. Murray, *Acc. Chem. Res.* 33 (2000) 27.

84. F. Caruso, R. A. Caruso, H. Mohwald, *Science* 282 (1998) 1111.

85. D. Losic, J. G. Shapter, J. J. Gooding, *Langmuir* 17 (2001) 3307.

86. P. Podsiadlo, B.S. Shim, N.A. Kotov, *Coordination Chem. Rev.* 253 (2009) 2835.

87. J. F. Silva, S. Griveau, C. Richard, J.H. Zagal, F. Bedioui, *Electrochem. Commun*. 9 (2007) 1629.

88. J.H. Zagal, S. Griveau, K.I. Ozoemena, T. Nyokong, F. Bedioui, *Nanosci. Nanotechnol.* 9 (2009) 2201.

89. J. Pillay, K. I. Ozoemena, *Electrochem. Commun*. 7 (2007) 1816.

90. J. Pillay, K.I. Ozoemena, *Electrochim. Acta 52 (2007) 3630.*

91. J. Pillay, K.I. Ozoemena, *Chem. Phys. Lett*. 441 (2007) 72.

92. K.I. Ozoemena, P. Westbroek, T. Nyokong, *Electrochem. Commun.* 3 (2001) 529.

93. K.I. Ozoemena, T. Nyokong, *Electrochim. Acta* 47 (2002) 4035.

94. B.O. Agboola, K.I. Ozoemena, *Phys.Chem.Chem.Phys.* 10 (2008) 2399.

95. K.I. Ozoemena, T. Nyokong, P. Westbroek, *Electroanalysis* 15 (2003) 1762.

96. V. Zucolotto, M. Ferreira, M.R. Cordeiro, C.J.L. Constantino, W.C. Moreira, O.N. Oliveira Jr., *Synth. Met.* 137 (2003) 945.

97. J.R. Siqueira Jr., L.H.S. Gasparotto, O.N. Oliveira Jr., V. Zucolotto, *J. Phys. Chem. C.* 112 (2008) 9050.

98. J.R. Siqueira Jr., L.H.S. Gasparotto, F.N. Crespilho, A.J.F. Carvalho, V. Zucolotto, O.N. Oliveira Jr., *J. Phys. Chem. B* 110 (2006) 22690.

99. J.R. Siqueira Jr., F.N. Crespilho, V. Zucolotto, O.N. Oliveira Jr., *Electrochem. Commun.* 9 (2007) 2676.

100. H. Benten, N. Kudo, H. Ohkita, S. Ito, *Thin Solid Films* 517 (2009) 2016.

101. M. Monthioux, V. L. Kuznetsov, *Carbon* 44 (2006) 1621.

102. L.V. Radushkevich, V.M Lukyanovich, *Zurn Fisic Chim.* 26 (1952) 88.

103. Hughes T.V, Chambers C.R. *US Patent 405480*, 1889.

104. S. Iijima, *Nature* 354 (1991) 56.

105. P.G. Wiles, J. Abrahamson, *Carbon* 16 (1978) 341.

106. T. W. Ebbesen, P.M. Ajayan, *Nature* 358 (1992) 220.

107. Y. Ando, S. IiJima, *Jpn. J. Appl. Phys.* 37 (1993) L107.

108. S. Ijima, T. Ichihashi, *Nature* 363 (1993) 603.

109. M. J. Yacaman, M. M. Yoshida, L. Rendon, J. G. Santiesteban, *Appl. Phys. Lett.* 62 (1993) 202.

110. A. Thess, R. Lee, P. Nikolaev, H. Dai, P. Petit, J. Robert, C. Xu, Y. H. Lee, S. G. Kim, A. G. Rinzler, D. T. Colbert, G. E. Scuseria, D. Tomane´k, J.E. Fischer, R.E. Smalley, *Science* 273 (1996) 483.

111. C.P. Poole Jr., F.J. Owens, *Introduction to Nanotechnology*, John Wiley and Sons Inc., Hoboken, New Jersey, 2003.

112. S.C. Lyu, T.J. Lee, C.W. Yang, J.C. Lee, *Chem. Comm.* 12 (2003) 1404.

113. C. E. Banks, R. G. Compton, *Analyst* 131 (2006) 15.

114. (a) The Nanotube site: http://nanotube.msu.edu:05/02/07. (b) J. Despres, E. Daguerre, K. Lafdi, *Carbon* 33 (1995) 87.

115. S. Iijima, C. Brabec, A. Maiti, J. Bernholc, *J. Chem. Phys.* 104 (1996) 2089.

116. B.I. Yakobson, C. J. Brabec, J. Bernholc, *Phys. Rev. Lett.* 76 (1996) 2511.

117. (a) J. Hone, M. Whitney, A. Zettle, *Synth. Met.* 103 (1999) 2498. (b) M. Burghard, *Surface Science Reports* 58 (2005) 1.

118. A.G. Rinzler, J.H. Hafner, P. Nikolaev, L. Lou, S.G. Kim, D. Tomanec, P. Nordlander, D.T. Colbert, R.E. Smalley, *Science* 269 (1995) 1550.

119. P. J. Britto, K. S. V. Santhanam, P. M. Ajayan, *Bioelectronics and Bioenergetics* 41 (1996) 121.

120. J.W.G. Wilder, L.C. Venema, A.G. Rinzler, R.E. Smalley, C. Dekker, *Nature* 391 (1998) 59.

121. T. Mühl, D. Elefant, A. Graff, R. Kozhuharova, A. Leonhardt, I. Mönch, M. Ritschel, P. Simon, S. Groudeva-Zotova, C.M. Schneider, *J. of Appl. Phys.* 93 (2003) 7894.

122. F. Cordella, M. Nardi, E. Menna, C. Hébert, M.A. Loi, *Carbon* 47 (2009) 1264.

123. V.N. Popov, *Materials Science and Engineering R* 43 (2004) 61.

124. C.Y Chen, T.C Chien, Y.C Chan, C.K. Lin, S.C. Wang, *Diamond and Related Materials* 18 (2009) 482.

125. S. Kawasaki, Y. Iwai, M. Hirose, *Carbon* 47 (2009) 1081.

126. J. Kong, N. R. Franklin, C. Zhou, M. G. Chapline, S. Peng, K. Cho, H. Dai, *Science* 287 (2000) 622.

127. R.A Jishi, M.S. Dresselhaus, G. Dresselhaus, *Matter and Materials Physics* 47 (1993) 16671.

128. M.S. Strano, C.A. Dyke, M.L. Usrey, P.W. Barone, M.J. Allen, H. Shan, C. Kittrell, R.H. Hauge, J.M. Tour, R.E. Smalley, *Science* 301 (2003) 1519.

129. C.N.R. Rao, A. Govindaraj, B.C. Satishkumar, *Chem. Commun.* 13 (1996) 1525.

130. E.T. Mickelson, I.W. Chiang , J.L. Ziammerman, P.J. Boul, J. Lozano , J. Liu, R.E. Smalley , R.H. Hauge , J.L. Margrave, *J. Phys. Chem. B*. 103 (1999) 4318.

131. J. Zhu, J.D. Kim, H.Q. Peng, J.L. Margrave, V.N. Khabashesku, E.V. Barrera, *Nano Lett.* 3 (2003) 1107.

132. P.J. Boul, J.Liu, E.T. Mickelson, C.B. Huffman, L.M. Ericson, I.W. Chiang, K.A. Smith, D.T. Colbert, R.H. Hauge, J.L. Margrave, R.E. Smalley, *Chem. Phys. Lett.* 310 (1999) 367.

133. B. Zhao, H. Hu, R.C. Haddon, *Adv. Funct. Mater.* 14 (2004) 71.

134. J. Chen, M.A. Hamon, H. Hu, Y. Chen, A.M. Rao, P.C. Eklund, R.C. Haddon, *Science* 282 (1998) 95.

135. R.H. Baughman, C. Cui, A.A. Zakhidov, Z. Iqbal, J.N. Barisci, G.M. Spinks, G.G. Wallace, A. Mazzoldi, D. De Rossi, A.G. Rinzler, O. Jaschinski, S. Roth, M. Kertesz, *Science* 284 (1999) 1340.

136. G.G. Wildgoose, C.E. Banks, H.C. Leventis, R.G. Compton, *Microchim Acta* 152 (2006)187.

137. G. Che, B.B. Lakshmi, E.R. Fisher, C.R. Martin, *Nature* 393 (2000) 346.

138. T. Matsumoto, T. Komatsu, H. Nakano, K. Arai, Y. Nagashima, E. Yoo, T. Yamazaki, M. Kijima, H. Shimizu, Y. Takasawa, J. Nakamura, *Catal. Today* 90 (2004) 277.

139. Z. Liu, X. Lin, J.Y. Lee,W. Zhang, M. Han, L.M. Gan, *Langmuir* 18 (2002) 4054.

140. W. Li, C. Liang, J. Qiu, W. Zhou, H. Han, Z. Wei, G. Sun, Q. Xin, *Carbon* 40 (2002) 787.

141. T. Matsumoto, T. Komatsu, K. Arai, T. Yamazaki, M. Kijima, H. Shimizu, Y. Takasawa, J. Nakamura, *Chem. Commun.* 7 (2004) 840.

142. N. Jha, A.L.M. Reddy, M.M. Shaijumon, N. Rajalakshmi, S. Ramaprabhu, *International Journal of Hydrogen Energy* 33 (2008) 427.

143. battery

144. Z. K. Tang, L. Zhang, N. Wang, X.X. Zhang, G.H. Wen, G.D. Li, J.N. Wang, C.T. Chan, P. Sheng, *Science* 292 (2001) 2462.

145. V. Gupta, N. Miura, *Electrochim. Acta* 52 (2006) 1721.

146. A.C. Dillon, K.M. Jones, T. A. Bekkedahl, C.H. King, D.S . Bethune, M.J . Heben, *Nature* 386 (1997) 377.

147. S.J . Tans, R.M. Verschueren, C. Dekker, *Nature* 393 (1998) 49.

148. J. M.Planeix, N.Coustel, B. Coq, V.Brotons, P.S. Kumbhar, R. Dutartre, P.Geneste, P.Bernier, P. M. Ajayan, *J. Am. Chem. Soc.* 116 (1994) 7935.

149. S.Saito, *Science* 278 (1997) 77.

150. P.Kim, C.M. Lieber, *Science* 286 (1999) 2148.

151. K.H. An, W.S. Kim, Y.S. Park, J.-M. Moon, D.J. Bae, S.C. Lim, Y.S. Lee, Y.H. Lee, *Adv. Funct. Mater.* 11 (2001) 387.

152. M.S. Dresselhaus, *Nature* 358 (1992) 195.

153. S.J. Tan, M.H. Devoret, H. Dai, A. Thess, R.E. Smalley, L.J. Geerligs, C. Dekker, *Nature* 386 (1997) 474.

154. A. Bianco, K. Kostarelos, C.D. Partidos, M. Prato, *Chem. Commun.* 5 (2005) 571.

155. K. Kostarelos, L. Lacerda, C.D. Partidos, M. Prato, A. Bianco, *J. Drug Deliv. Sci. Technol.* 15 (2005) 41.

156. N.W.S. Kam, Z. Liu, H. Dai, *J. Am. Chem. Soc.* 127 (2005) 12492.

157. A. Bianco, K. Kostarelos, M. Prato, *Curr. Opin. Chem. Biol.* 9 (2005) 674.

158. X. Yu, R. Rajamani, K.A. Stelson, T. Cui, *Sensors and Actuators* 132 (2006) 626.

159. Y. Shingaya, T. Nakayama, M. Aono, *Physica B* 323 (2002) 153.

160. Ph. Avouris, R. Martel, V. Derycke, J. Appenzeller, *Physica B* 323 (2002) 6.

161. J.Kong, N.R. Franklin, C. Zhou, M.G. Chapline, S. Peng, K. Cho, H. Dai, *Science* 287 (2000) 622.

162. J. Kong, M.G. Chapline, H.Dai, *Adv. Mater.* 13 (2001) 1384.

163. P.G. Collins, K. Bradley, M. Ishigami, A. Zettl, *Science* 287 (2000) 1801.

164. A. Qureshi, W.P. Kang, J.L. Davidson, Y. Gurbuz, *Diamond and Related Materials* (2008) doi:10.1016/j.diamond.2009.09.008.

165. P.J. Britto, K.S.V. Santhanam, A. Rubio, J.A. Alonso, P.M. Ajayan, *Adv. Mater.* 11 (1999) 154.

166. J. J. Davis, R.J. Coles, H. A.O. Hill, *J. Electroanal. Chem*. 440 (1997) 279.

167. H. Luo, Z. Shi, N. Li, Z. Gu, Q. Zhuang, *Anal. Chem.* 73 (2001) 915.

168. G. Che, B.B. Lakshmi, E.R. Fisher, C.R. Martin, *Nature* 393 (1998) 346.

169. F. Valentini, A. Amine, S. Orlanducci, M. Letiziu, G. Palleschi, *Anal. Chem.* 75 (2003) 5413.

170. Z. Di- Zhao, W.De Zhang, H. Chen, Q. M. Luo, *Talanta* 58 (2002) 529.

171. J.J. Gooding, R. Wibowo, J. Liu, W. Yang, D. Losic, S. Orbons, F.J. Mearns, J.G. Shapter, D.B. Hibbert, *J. Am. Chem. Soc.* 125 (2003) 9006.

172. J. Wang, M. Li, Z. Shi, N. Li, Z. Gu, *Microchim. J.* 73 (2002) 325.

173. J. Wang, M. Li, Z. Shi, N. Li, Z. Gu, *Electrochim. Acta* 47 (2001) 651.

174. F.H. Wu, G.C. Zhao, X.W. Wei, *Electrochem. Commun.* 4 (2002) 690.

175. M. Musameh, J. Wang, A. Merkoci, Y. Lin, *Electrochem. Commun.* 4 (2002) 743.

176. K. Wu, J. Fei, S. Hu, *Anal. Biochem.* 318 (2003) 100.

177. K.B. Malea, S. Hrapovica, Y. Liua, D. Wang, J.H.T. Luong, *Anal. Chim. Acta* 516 (2004) 35.

178. C. Yang, *Anal. Sci.* 20 (2004) 821.

179. G-Q Zhang, X-G Zhang, Y-G Wang, *Carbon* 42 (2004) 3097.

180. N.S. Lawrence, R.P. Deo, J. Wang, *Talanta* 63 (2004) 443.

181. J. Wang, M. Musameh, *Anal. Chimica Acta* 511 (2004) 33.

182. J. Wang, S.B. Hocevar, B. Ogorevc, *Electrochem. Commun*. 6 (2004) 176.

183. M.L. Pedano, G.A. Rivas, *Electrochem. Commun*. 6 (2004) 10.

184. J-S Yea, Y. Wen, W.D. Zhang, L.M. Gan, G-Q Xu, F-S Sheu, *Electrochem. Commun*. 6 (2004) 66.

185. R.P. Deo, J. Wang, I. Block, A. Mulchandani, K.A. Joshi, M. Trojanowicz, F. Scholz, W. Chen, Y. Lin, *Anal. Chim. Acta* 530 (2005) 185.

186. N.S. Lawrence, R.P. Deo, J. Wang, *Electroanalysis* 17 (2005) 65.

187. D. Nkosi, K.I. Ozoemena, *J. Electroanal. Chem.* 621 (2008) 304.

188. F.C. Moraesa, L.H. Mascaroa, S.A.S. Machadob, C.M.A. Brett, *Talanta* 79 (2009) 1406.

189. V. Selvaraj, M. Alagar, K. S. Kumar, *Appl. Catal. B: Environ.* 75 (2007) 129.

190. A. Salimi, C.E. Banks, R.G. Compton, *Analyst* 129 (2004) 225.

191. D.A. Geraldo, C.A. Togo, J. Limson, T. Nyokong, *Electrochim. Acta*, 53 (2008) 8051.

192. T. Mugadza, T. Nyokong, *Electrochim. Acta* 54 (2009) 6347.

193. K.I. Ozoemena, J. Pillay, T. Nyokong, *Electrochem. Commun.* 8 (2006) 1391.

194. M.P. Siswana, K.I. Ozoemena, T. Nyokong, *Electrochim. Acta* 52 (2006) 114.

195. D. Nkosi, K.I. Ozoemena, *Electrochim. Acta* 53 (2008) 2782.

196. B. O. Agboola, S.L. Vilakazi, K. I. Ozoemena *J. Solid State Electrochem.* 13 (2009) 1367.

197. A.S. Adekunle, K.I. Ozoemena, *Electrochim. Acta* 53 (2008) 5774.

198. A.S. Adekunle, K.I. Ozoemena, *J. Solid State Electrochem.* 12 (2008) 1325.

199. A.S. Adekunle, J. Pillay, K. I. Ozoemena, *Electroanalysis* 20 (2008) 2587.

200. K. I. Ozoemena, D. Nkosi, J. Pillay, *Electrochim. Acta* 53 (2008) 2844.

201. A. Braun, J. Tcherniac, *Berichte der Deutschen Chemischen Gesellschaft* 40 (1907) 2709.

202. H. de Diesbach, E. von der Weid, *Helevtica Chimica Act* 10 (1927) 886.

203. P.Gregory, *J. Porphyrins Phthalocyanines* 3 (1999) 468.

204. R.P. Linstead, *J. Chem. Soc.* (1934) 1016.

205. J.M. Roberston, *J. Chem. Soc.* (1935) 615.

206. J.M. Roberston, *J. Chem. Soc.* (1936) 1195.

207. *Phthalocyanines: Properties and Applications,* C.C. Leznoff and A.B.P.Lever, Eds., VCH Publishers, New York, Vols. 1-4, 1989, 1993, 1993, 1996.

208. E.Ough, T. Nyokong, K.A.M. Creber, M.J. Stillman, *Inorg. Chem.* 27 (1988) 2725.

209. R.B. Linstead, A.R. Lowe, *J. Chem. Soc.* (1934) 1022.

210. J.H. Zagal, *Coord. Chem. Rev.* 119 (1992) 89.

211. C.B. Murray, D.J. Norris, M.G. Bawendi, *J. Am. Chem. Soc.* 115 (1993) 8706.

212. B.O. Dabbousi, M.G. Bawendi, O. Onitsuka, M.F. Rubner, *Appl. Phys. Lett.* 66 (1995) 1316.

213. T. Enokida, R. Hirohashi, S. Mizukami, *J. Imaging Sci.* 35 (1991) 235.

214. T. Saito, T. Kawanishi, A. Kakuta, *Jpn. J. Appl. Phys. A* 30 (1991) L1182.

215. Y. Wang, K. Deng, L. Gui, Y. Tang, J. Zhou, L. Cai, J. Qiu, D. Ren and Y. Wang, *J. Colloid Interface Sci.* 213 (1999) 270.

216. G. de la Torre, C.G. Claessens, T. Torres, *Chem. Commun.* (2007) 2000.

217. R.K. Sen, J. Zagal, E. Yerger, *Inorg. Chem*. 16 (1977) 3379.

218. J. Limson, T. Nyokong, *Electroanalysis* 9 (1997) 255.

219. K. Hanabusa, H. Sharai in: A.P.B. Lever and C.C. Leznoff (Eds.), *Phthalocyanines: Properties and Applications*, VHC Publishers, New York, 1993, Vol.2.

220. H. Kasuga in: A.P.B. Leverand C.C. Leznoff (Eds.), *Phthalocyanine: Properties and Applications,* VCH Publishers, New York, 1996, Vol.4.

221. M. Thamae, T. Nyokong, *J. Electroanal. Chem*. 470 (1999) 126.

222. K. Morishige, S. Tomoyasu, G. Iwano, *Langmuir* 13 (1997) 5184.

223. A.W. Snow, W.R. Barger in: A.P.B. Lever and C.C. Leznoff (Eds.), *Phthalocyanines: Properties and Applications*, VCH Publishers, New York, 1989, Vol.1.

224. E. Ben-Hur, I. Rosenthal, *Int. J. Radiat. Biol*. 47 (1985) 145.

225. E. Ben-Hur, I. Rosenthal, *J. Photochem. Photobiol*. 42 (1985) 129.

226. I. Rosenthal, E. Ben-Hur in: A.P.B. Lever and C.C. Leznoff *Phthalocyanine: Properties and Applications,* VCH Publishers, New York, 1989, Vol.1.

227. D. Phillips, *Pure Appl. Chem*. 67 (1995) 117.

228. I.J. MacDonald, T. Dougherty, *J. Porphyrins Phthalocyanines* 5 (2001) 105.

229. P. Gregory, *J. Porphyrins Phthalocyanines* 3 (1999) 468.

230. P. Gregory in: *High Technology Applications of Organic Colorants*, Plenum Press, New York, 1991.

231. N.B. McKeown, *Chem. Ind*. (1999) 92.

232. G.C.S. Collins, D.J. Schiffrin, *J. Electroanal. Chem*. 139 (1982) 335.

233. M.M. Nicholson in: A.P.B.Lever and C.C. Leznoff (Eds.), *Phthalocyanine: Properties and Applications*, VCH Publishers, New York, 1993. Vol. 3.

234. N. Toshina, T. Tominaga, *Bull. Chem. Soc. Jpn.* 69 (1996) 2111.

235. J.E. Kuder, *J. Imaging Sci*. 32 (1988) 51.

236. R. Ao, L. Kummert, D. Haarer, *Adv. Mater*. 5 (1995) 495.

237. S. Nalwa, J.A. Shirk in: A.P.B. Lever and C.C. Leznoff (Eds.), *Phthalocyanine: Properties and Applications,* VCH Publishers, New York, 1993, Vol. 4.

238. D.K.P. Ng, Y-O Yeung, W.K. Chan, S-C Yu, *Tet. Lett*. 38 (1997) 6701.

239. D. Worhle, D. Meissener, *Adv. Mater*. 3 (1991) 129.

240. D. Worhle, L. Kreienhoop, D. Schlettwein in: A.P.B. Lever and C.C. Leznoff (Eds.), *Phthalocyanine: Properties and Applications*, VCH Publishers, New York, 1996, Vol.4.

241. A.B.P. Lever, M.R. Hempstead, C.C. Leznoff, W. Lui, M. Melnik, W.A. Nevin, P. Seymour, *Pure Appl. Chem*. 58 (1986) 1467.

242. B. Simic-Glavaski in: A.P.B. Lever and C.C. Leznoff (Eds.), *Phthalocyanine: Properties and Applications*, VCH Publishers, New York, 1993, Vol.3.

243. J. Simon, J.J. Andre, *Mol. Semicond.*, Springer, Berlin, 1985.

244. J. Simon, T. Toupance in: D.N. Reinhoudt (Ed.), *Comprehensive Supramolecular Chemistry Vol.10*, Pergamon, London, 1996.

245. M. Iwamoto, *J. Mater. Chem*. 10 (2000) 99.

246. P. Vasuvedan, N. Poughat, A.K. Shuklat, *Appl. Organomet. Chem*. (1996) 591.

247. M. Thamae, T. Nyokong, *J. Electroanal. Chem*. 470 (1999) 126.

248. E. Ben-Hur, I. Rosenthal, *Int. J. Radiat. Biol*. 47 (1985) 145.

249. D. Phillips, *Pure Appl. Chem*. 67 (1995) 117.

250. Y. Lu, R.G. Reddy, *Electrochim. Acta* 52 (2007) 2562.

251. N. Martz, C. Roth, H. Fueb, *J. Appl. Electrochem*. 35 (2005) 85.

252. K.I. Ozoemena, T. Nyokong, in: C. A Grimes, E.C. Dickey, M.V. Pishko, (Eds.), *Encyclopedia of Sensors Vol.3, Chapter E, pp.157 – 200*, American Scientific Publishers, California, 2006.

253. M. Siswana, K.I. Ozoemena, T. Nyokong, *Talanta* 69 (2006) 1136.

254. S.A. Mamuru, K.I. Ozoemena, *Mat. Chem. Phys.* 114 (2009) 113.

255. G. Savage, *Glass and Glassware*; Octopus Books: London, 1975.

256. G. Lussac, *Annalen der Physik* 101(1832) 629.

257. M. Faraday, *Philos. Trans.* 147 (1857) 145.

258. J. Kunckels, *Nuetliche Observationes oder Anmerkungen von Auro und Argento Potabili*; Schutzens: Hamburg, 1676.

259. T. Graham, *Philos. Trans. R. Soc*. 151 (1861) 183.

260. N. Taniguchi, "*On the Basic Concept of 'Nano-Technology'*," Proc. Intl. Conf. Prod. Eng. Tokyo, Part II, Japan Society of Precision Engineering, 1974

261. S. Chen, R.W. Murray, *Langmuir* 15 (1999) 682.

262. A.C. Templeton, M.J. Hostetler, C.T. Kraft, R.W. Murray, *J. Am. Chem. Soc.* 120 (1998) 1906.

263. M. Brust, M. Walker, D. Bethell, D. J. Schiffrin, R. Whyman, *J. Chem. Soc. Chem. Commun.* 7 (1994) 801.

264. B. V. Enustun, J. Turkevich, *J. Am. Chem. Soc.* 85 (1963) 3317.

265. C.-C. You, A. Chompoosor, V.M. Rotello, *Nanotoday* 2 (2007) 34.

266. A. Verma, V.M. Rotello, *Chem. Commun.* 3 (2005) 303.

267. M.H. Rashid, R.R. Bhattacharjee, A. Kotal, T.K. Mandal, *Langmuir* 22 (2006) 7141.

268. L. N. Lewis, *Chem. Rev.* 93 (1993) 2693.

269. S. Guo, E. Wang, *Anal. Chim. Acta* 598 (2007) 181.

270. M-C. Daniel, D. Astruc, *Chem. Rev.* 104 (2004) 293.

271. G. Schmid, R. Pfeil, R. Boese, F. Bandermann, S. Meyers, G.H.M. Calis, W.A. Vandervelden, *Chem. Ber.* 114 (1981) 3634.

272. D. Bethell, M. Brust, D.J. Schiffrin, C. Kiely, *J. Electroanal. Chem.* 409 (1996) 137.

273. R.S. Ingram, R.W. Murray, *Langmuir* 14 (1998) 4115.

274. J.J. Pietron, R.W. Murray, *J. Phys. Chem. B* 103 (1999) 4440.

275. C.J. Zhong, W.X. Zheng, F.L. Leibowitz, *Electrochem. Commun.* 1 (1999) 72.

276. M.D. Musick, D.J. Pena, S.L. Botsko, T.M. McEvoy, J.N. Richardson, M.J. Natan, *Langmuir* 15 (1999) 844.

277. X.Y. Hu, Y. Xiao, H.Y. Chen, *J. Electroanal. Chem.* 466 (1999) 26.

278. S. Chen, *J. Phys. Chem. B* 104 (2000) 663.

279. J.F. Hicks, F.P. Zamborini, R.W. Murray, *J. Phys. Chem. B* 106 (2002) 7751.

280. S. Bharathi, M. Nogami, S. Ikeda, *Langmuir* 17 (2001) 1.

281. M.M. Maye, J. Luo, Y. Lin, M.H. Engelhard, M. Hepel, C.-J Zhang, *Langmuir* 19 (2003) 125.

282. M. Yang, Z. Zhang, *Electrochim. Acta* 49 (2004) 5089.

283. A. Toyota, N. Nakashima, T. Sagara, *J. Electroanal. Chem.* 565 (2004) 335.

284. P.S. Jensen, Q. Chi, F.B. Grumsen, J.M. Abad, A. Horsewell, D.J. Schiffrin, J. Ulstrup, *J. Phys. Chem. C* 111 (2007) 6124.

285. P. Ahonen, V. Ruiz, K. Kontturi, P. Liljeroth, B. M. Quinn, *J. Phys. Chem. C* 112 (2008) 2724.

286. A. S. Nair, K. Kimura, *Langmuir* 25 (2009) 1750.

287. T. R. Tshikhudo, D. Demuru, Z. Wang, M. Brust, A. Secchi, A. Arduini and A. Pochini, *Angew. Chem. Int. Ed.* 44 (2005) 2.

288. P. Hern´andez, I. S´anchez, F. Pat´on, L. Hern´andez, *Talanta* 46 (1998) 985.

289. J. O. Schenk, E. Milker, R. N. Adam, *J. Chem. Educ.* 60 (1983) 311.

290. Q.M. Xue, *Physiological and Pathological Chemistry of Nervous System*, Science Press, Beijing, 1978.

291. D. Voet, J.G. Voet, *Biochemistry 3rd ed.*, John Wiley & Sons, Hoboken, 2004, pp.659 and 664–666.

292. O. Gyllenhaal, L. Johansson, J. Vessman, *J. Chromatography A* 190 (1980) 347.

293. H.G. Lovelady, L.L. Foster, *J. Chromatography A* 108 (1975) 43.

294. L.Y. Zhang, S.F. Qv, Z.L. Wang, J.K Cheng, *J. Chromatogr. B* 792 (2003) 381.

295. S.L. Wei, G.Q. Song, J.M. Li, *J. Chromatogr. A* 166 (2005) 1098.

296. M.H. Sorouraddin, J.L. Manzoori, E. Kargarzadeh, *J. Pharm. Biomed.* 18 (1998) 877.

297. M. Zhu, X.M. Huang, J. Li, *Anal. Chim. Acta* 357 (1997) 261.

298. Y.Y. Su, J. Wang, G.N. Chen, *Talanta* 65 (2005) 531.

299. J. Michalowski, P. Halaburda, *Talanta* 55 (2001) 1165.

300. E.M. Garrido, J.L. Lima, D.M. Cristina, *J. Pharm. Biomed.* 15 (1997) 845.

301. J.X. Du, L.H. Shen, J.R. Lu, *Anal. Chim. Acta* 489 (2003) 183.

302. Z. Yang, G. Hu, X. Chen, J. Zhao, G. Zhao, *Colloids Surf. B: Biointerf.* 54 (2007) 230.

303. H.S. Wang, D-Q. Huang, R-M. Liu, *J. Electroanal. Chem.* 570 (2004) 83.

304. J. Gong, X. Lin, *Electrochim. Acta* 49 (2004) 4351.

305. W. Ren, H.Q. Luo, N.B. Li, *Biosens. Bioelectron.* 21 (2006) 1086.

306. N.B. Li, W. Ren, H.Q. Luo, *Anal. Chim. Acta* 378 (1999) 151.

307. M. Marazuela, L. Agui, A. Gonzalez-Cortes, P. Yanez-Sedeno, J.M. Pingarro, *Electroanalysis* 11 (1999) 1333.

308. F. Valentini, G. Palleschi, E. Lopez Morales, S. Orlanducci, E. Tamburri, M. L. Terranova, *Electroanalysis* 19 (2007) 859

309. Z. Guo, S. Dong, *Electroanalysis* 17 (2005) 607.

310. S.L. Jewett, S. Eggling, L. Geller, *J. Inorg. Biochem* 66 (1997) 165.

311. C.E. Sanger-van de Griend, A.G. Ek, M.E. Widahl-Nasman, E.K.M.J. Andersson, *Pharm. Biomed. Anal.* 41 (2006) 77.

312. E.L. Ciolkowski, K.M. Maness, P.S. Cahlil, R.M. Wightman, *Anal. Chem.* 66 (1994) 3611.

313. J. Wang, P. Tuzhi, T. Golden, *Anal. Chim. Acta* 194 (1987) 129.

314. J. Ni, H. Ju, H. Chen, D. Leech, *Anal. Chim. Acta* 378 (1999) 151.

315. H. Zhang, X. Zhou, R. Hui, N. Li, D. Liu, *Talanta* 56 (2002) 1081.

316. L.J. Thenard, *Annales de chimie et de physique* 8 (1818) 308.

317. C.A. Gervasi, P.E. Alvarez, M.V. Fiori Bimbi, M.E. Folquer, *J. Electroanal. Chem.* 601 (2007) 194.

318. M. Knoll, *Zeitschrift für technische Physik* 16 (1935) 467.

319. M. von Ardenne, *Zeitschrift für Physik* 108 (1938) 553.

320. M von Ardenne, *Zeitschrift für technische Physik* 19 (1938) 407.

321. P.E. Alvarez, S.B. Ribotta, M.E. Folquer, C.A. Gervasi, J.R. Vilche, *Corros. Sci*. 44 (2002) 49.

322. J. B. Hudson, *Surface Science: An Introduction*, John Wiley & Sons, New York, 1998.

323. M.H. Kibel, in: D. J. O'Connor, B.A. Sexton, R. St. C. Smart, (Eds.), *Surface Analysis Methods in Material Science*, Springer-Verlag, Berlin Heidelberg, Germany, 1993.

324. X. Jiang, T. Wang, *Applied Surface Science* 252 (2006) 8029.

325. G. Binnig, C.F. Quate, C. Gerber, *Phys. Rev. Lett.* 56 (1986) 930.

326. E. Le Bourhis, G. Patriarche, *Micron* 38 (2007) 377.

327. C.S. Pande, S. Smith, L.E. Richards, in: G.W. Bailey (Ed.), *Proceedings of 43rd Annual Meeting of Electron Microscopy Society of America*, San Francisco Press Inc., San Francisco, CA, 1985.